S-IgA and IgG standards for each IAV subtypes are not commercially available, the concentrations of anti-IAV-specific antibody in the nasopharyngeal specimens and sera were determined from the standard regression curves with human IgA and IgG of known concentrations in a human IgA and IgG quantitation kits (Bethyl Laboratories Inc., Montgomery, TX). The relative values of anti-IAV-specific S-IgA and IgG were expressed as units (U); one U of each anti-IAV-specific S-IgA and IgG was determined from the regression curves as the point corresponding to 1 μg of human IgA and 1 mg of human IgG detected in the assay system, respectively, as described previously [13,17]. Since the concentration of nasal wash samples varies widely between individuals depending on the aspiration efficiency and patient age, the concentration of anti-IAV-specific S-IgA (U/mL) was normalized by the amount of protein (mg/mL). Since there was no significant variability in serum protein concentrations, the row values of anti-IAV-specific IgG concentrations (U/mL) were used. The protein concentrations in the nasopharyngeal specimens were measured using a bicinchoninic acid protein assay reagent kit (Pierce, Rockford, IL).

Statistical analysis

Results are presented as the median (interquartile range), or numbers (%) of observations. The S-IgA levels in nasopharyngeal specimens of the different patient groups were compared by the Mann-Whitney U-test and Wilcoxon signed-rank test. Between group comparisons of disease symptoms were made using Fisher's exact test with the Bonferroni correction. A P value <0.05 was considered statistically significant.

Results

Patient characteristics

Table 1 lists the characteristics of patients of the five groups. The most common features of influenza were fever (defined as body temperature ≥38°C), sore throat, cough, nasal discharge, headache and body aches. About half (48.6–64.7%) of the patients in each group had received vaccination before the onset of the influenza season and no significant differences in the values were observed among the five groups. The prevalence of disease signs and symptoms at admission to hospital was similar among the five groups. The time between onset of illness and initial examination ranged from 1.0 to 1.9 days with a mean value of 1.7±0.6 days.

Effects of OSV and ZNV on nasopharyngeal antiviral-S-IgA production and serum antiviral-IgG in patients treated with or without CAM

Table 2 summarizes the levels of anti-IAV(H1N1)- and (H3N2)-specific S-IgA (U/mg protein) and total S-IgA (μg/mg protein) before and 5 days after treatment with OSV and ZNV, with or without CAM. In the control (no treatment) group, significant increases in the concentrations of anti-IAV-specific S-IgA against subtypes H1N1 ($P<0.05$) and H3N2 ($P<0.01$) were observed at 5 days after infection. The percentages of patients with greater than or equal (≥1-fold) to baseline titer before treatment and greater than or equal to a four-fold increase (≥4-fold) from baseline titer in the no-treatment group against subtype H1N1 were 61.5 and 26.2, respectively, and against subtype H3N2 were 69.2 and 15.4, respectively. Treatment with OSV and ZNV significantly suppressed the percentage of patients with ≥1-fold of baseline titer against both H1N1 and H3N2 subtypes, compared with the values in the no-treatment group. However, co-administration of CAM and OSV boosted S-IgA induction and increased the percentage of patients with ≥1-fold of baseline titer from 42.9 to 65.0 against H1N1 and from 42.9 to 70.0 against H3N2 (P value versus OSV group for H1N1: $P<0.06$ to <0.09, H3N2: <0.05). Co-administration of CAM and ZNV resulted in mild restoration of the suppressed percentage of patients with ≥1-fold of baseline titer from 37.0 to 50.0 against H1N1 and from 48.1 to 60.0 against H3N2, although the differences between the two were not statistically significant. There were no significant differences in the percentages of patients with ≥4-fold of baseline S-IgA titer among the five treatment groups.

Table 3 lists the levels of serum anti-IAV(H1N1)- and (H3N2)-specific IgG (U/mL) and total IgG (mg/mL) before and 5 days after treatment of IAV infection with OSV and ZNV, with or without CAM. Significant increases were noted in serum levels of anti-IAV-specific IgG in all groups at 5 days after treatment, except those against H1N1 in the OSV and ZNV groups. In particular, ZNV treatment significantly reduced the percentage of patients with ≥1-fold of baseline titer against H1N1 compared with the no-treatment group, from 73.5 to 40.9 ($P<0.01$), in a manner similar to that noted in mucosal S-IgA responses. In addition, the combination of CAM plus ZNV significantly increased the percentage of patients with ≥1-fold of baseline titer against H1N1 ($P<0.01$), though the increase against H3N2 was

Table 1. Patient characteristics.

	All patients	No Treatment	OSV	OSV+CAM	ZNV	ZNV+CAM
	(n=195)	(n=68)	(n=70)	(n=20)	(n=27)	(n=10)
Age, years, (range)*	5.9±3.3 (0–14)	7.3±3.9 (0–14)	4.2±2.7 (0–10)	5.1±2.1 (1–9)	7.0±1.6 (5–9)	6.9±2.0 (4–9)
Time between onset illness and initial examination (days)*	1.7±0.6	1.6±0.7	1.7±0.6	1.9±0.6	1.6±0.6	1.0±0.7
Previous vaccination (%)	112(57.4)	44(64.7)	34(48.6)	12(60.0)	17(63.0)	5(50.0)
Fever (%)	180(95.2)	63(92.6)	68(100)	16(88.9)	25(96.2)	8(88.9)
Sore throat (%)	68(35.4)	24(35.3)	20(29.9)	4(20.0)	15(55.6)	5(50.0)
Cough (%)	173(88.7)	64(94.1)	61(87.1)	16(80.0)	23(85.2)	9(90.0)
Nasal discharge (%)	177(90.8)	67(98.5)	64(91.4)	17(85.0)	20(74.1)	9(90.0)
Headache (%)	70(36.6)	26(38.2)	20(30.3)	4(20.0)	14(51.9)	6(60.0)
Body aches (%)	54(28.7)	16(23.5)	24(37.5)	3(15.8)	8(29.6)	3(30.0)

*Data are mean±SD.

doi:10.1371/journal.pone.0070060.t001

Table 2. Changes in anti-IAV-specific S-IgA production in untreated patients and patients treated with OSV and ZNV for 5 days, with or without CAM.

Treatment	n	S-IgA concentration						Percentage of patients with ≥1-fold and ≥4-fold increases in anti-IAV-specific S-IgA concentration during treatment			
		Anti-IAV-specific S-IgA (U/mg protein)				Total S-IgA (μg/mg protein)					
		H1N1		H3N2				H1N1		H3N2	
		Before	After	Before	After	Before	After	≥1-fold (After/before)	≥4-fold (After/before)	≥1-fold (After/before)	≥4-fold (After/before)
No treatment	65	2.3 (0.5–5.7)	3.1 (1.2–7.8)*	2.2 (0.6–3.8)	3.1 (1.0–6.7)¶	120.6 (90.3–177)	143.5 (118–204)*	61.5	26.2	69.2	15.4
OSV	70	1.3 (0.6–5.9)	1.2 (0.4–5.0)	1.0 (0.4–2.8)	1.1 (0.5–3.1)	122.8 (79.1–147)	128.0 (82.8–163)	42.9§	18.6	42.9‡	14.3
OSV+CAM	20	0.9 (0.3–1.4)	1.9 (0.3–12.3)*¶	0.7 (0.2–1.7)	1.5 (0.3–7.6) ¶	121.6 (74.1–153)	134.1 (98.9–214)*	65.0#†	30.0	70.0†	20.0
ZNV	27	3.8 (1.7–12.3)	4.5 (0.5–15.8)	2.0 (1.4–3.8)	2.6 (0.5–7.8)	109.7 (86.8–181)	149.8 (101–216)	37.0§	18.5	48.1§	11.1
ZNV+CAM	10	2.0 (1.6–7.1)	6.3 (2.2–19.5)	1.7 (1.2–2.4)	4.3 (1.8–11.6)	143.3 (104–202)	173.2 (151–207)	50.0	30.0	60.0	30.0

Data are median (interquartile range). Before and after denote before and after treatment, respectively.
*$P<0.05$,
¶$P<0.01$, versus before treatment for the same parameter (Wilcoxon signed-ranks test).
§$P<0.05$, versus the respective no treatment (Fisher's exact test). ‡$P<0.01$, versus the respective no treatment (Fisher's exact test).
#$P<0.06$ to <0.09, versus the OSV group (Fisher's exact test). †$P<0.05$, versus the OSV group (Fisher's exact test).
doi:10.1371/journal.pone.0070060.t002

Table 3. Changes in anti-IAV-specific IgG production in untreated patients and patients treated with OSV and ZNV for 5 days, with or without CAM.

Treatment	n	IgG concentration						Percentage of patients with ≥1-fold and ≥4-fold increases in anti-IAV-specific IgG concentration during treatment			
		Anti-IAV-specific IgG (U/mL)				Total IgG (mg/mL)					
		H1N1		H3N2				H1N1		H3N2	
		Before	After	Before	After	Before	After	≥1-fold (After/before)	≥4-fold (After/before)	≥1-fold (After/before)	≥4-fold (After/before)
No treatment	49	0.5 (0.2–0.9)	0.8 (0.4–1.5)¶	0.4 (0.2–0.7)	0.8 (0.3–1.4)¶	19.3 (10.9–48.3)	17.7 (10.2–28.1)*	73.5	30.6	73.5	34.7
OSV	52	0.2 (0.03–0.7)	0.5 (0.06–1.0)	0.2 (0.04–0.5)	0.4 (0.06–1.1)¶	13.2 (9.1–17.6)	11.8 (8.6–17.4)	63.5	21.2	75.0	32.7
OSV+CAM	14	0.5 (0.3–0.6)	0.9 (0.5–1.4)¶	0.5 (0.2–0.5)	0.6 (0.4–1.2)*	14.1 (10.1–21.1)	12.0 (9.6–16.7)	78.6	21.4	85.7	14.3
ZNV	22	0.6 (0.3–1.1)	0.6 (0.4–1.1)	0.3 (0.2–0.5)	0.5 (0.4–0.9)¶	11.9 (8.3–31.4)	15.3 (9.4–28.4)	40.9‡	13.6	68.2	18.2
ZNV+CAM	8	0.3 (0.2–0.6)	0.9 (0.2–1.8)*	0.4 (0.2–0.7)	1.4 (0.4–2.6)*	15.4 (10.2–22.0)	12.0 (8.9–14.9)	100.0†	25.0	100.0#	50.0

Data are median (interquartile range). Before and after denote before and after treatment, respectively.
*$P<0.05$,
¶$P<0.01$, versus before treatment for the same parameter (Wilcoxon signed-ranks test).
‡$P<0.01$, versus the respective no treatment (Fisher's exact test).
#$P<0.06$ to <0.09, versus the ZNV group (Fisher's exact test).
†$P<0.01$, versus the ZNV group (Fisher's exact test).
doi:10.1371/journal.pone.0070060.t003

marginal, ($P<0.06$ to <0.09), compared with ZNV alone. There were no significant differences in the percentages of patients with ≥4-fold of baseline IgG titer among the five treatment groups.

Table 4 compares the prevalence of disease manifestations at day 5 after treatment. Significant improvements were noted in the prevalence of cough in the OSV+CAM group, compared with the OSV group ($P<0.05$), and nasal discharge in the ZNV+CAM group, compared with the ZNV group ($P<0.05$). However, there were no significant differences in the effects of various treatments on the other listed symptoms among the five treatment groups.

Frequency of re-infection in subsequent year

Based on the low level of acquired mucosal anti-IAV-specific S-IgA after infection, patients were at risk of re-infection in the subsequent year, particularly those treated with OSV or ZNV. Figure 1 lists the percentages of re-infected individuals according to the treatment received in the preceding year. The IAV pH1N12009 was the predominant circulating virus in Japan with a peak during October-December of 2009. Even under the spread of a new virus subtype in the 2009/2010, only 8.6% of the children of the no-treatment group were re-infected. However, the proportions of children treated the previous year with OSV and ZNV who developed re-infection in 2009–2010 were significantly higher at 37.3% and 45.0%, respectively ($P<0.01$), than those of the no-treatment group. The combination treatment of CAM plus OSV and CAM plus ZNV tended to reduce the re-infection rate to 17.6% and 22.2%, respectively, albeit insignificantly.

Discussion

The main findings of the present study were the following: (i) Treatment with antiviral neuraminidase inhibitors, OSV and ZNV, tended to suppress the production of respiratory anti-IAV-specific S-IgA as well as systemic anti-IAV-specific IgG in pediatric patients with influenza. (ii) The combination treatment of CAM plus OSV or ZNV mildly or significantly enhanced the production of anti-IAV S-IgA in the nasopharyngeal specimens and/or anti-IAV IgG in sera and tended to restore the suppressed local mucosal and systemic immunity observed with antiviral inhibitor agents. (iii) The rates of IAV re-infection in the subsequent year were significantly higher for the OSV and ZNV groups than the control group, whereas the combination of CAM plus OSV or ZNV tended to reduce such rate.

There is general agreement that the first line of host defense against infection is mucosal immunity, particularly nasopharyngeal immunity, which constitutes a major component of the immunological humoral and cell-mediated responses in the upper and lower respiratory tracts [18,19]. However, the currently available intramuscularly and subcutaneously-injected influenza vaccines predominantly induce systemic IgG but not S-IgA and weak cellular immunity in the airway mucosa [18–21]. In fact, the levels of anti-IAV S-IgA relative to the total sIgA were low in nasal washes of all influenza patients on admission, whereas serum levels of anti-IAV IgG levels varied widely, probably reflecting the history of infection and vaccination in these individuals [13,17]. Treatment of pediatric influenza with OSV or ZNV for 5 days significantly suppressed acquired anti-IAV S-IgA levels in nasal washes (Table 2) and these changes may also explain the higher frequency of re-infection in the OSV and ZNV groups in the subsequent year (Figure 1). The results may be supported by previous findings that mucosal S-IgA is primarily involved in cross-protection of the mucosal surface against variant IAV infection, and the mechanism of broad-spectrum cross-protection could be explained by the wide-range cross-reactivity of S-IgA [22–25].

The suppressive effects of OSV and ZNV on mucosal anti-IAV S-IgA levels, probably due to diminution of viral antigen production by anti-viral neuraminidase inhibitors, seem to be ameliorated by co-administration of CAM. CAM boosted mucosal and/or systemic immunity and tended to increase the levels of anti-IAV S-IgA in nasal washes and IgG in serum in the OSV- and ZNV-treated patients (Tables 2 and 3). This effect of CAM resulted in an increase in the percentage of patients with ≥1-fold of baseline titer before treatment, particularly S-IgA in the OSV-treated patients and IgG in the ZNV-treated patients. Although patients of the ZNV group were slightly older (about 2 years) than those of the OSV group, because of age limitation of oral inhalation of ZNV powder, the observed effects of ZNV on mucosal and systemic immunity were similar to those of OSV with or without CAM. The effects of OSV and ZNV with or without CAM could be clearer in naïve children with low or undetectable pre-existing immunological memory. The present results emphasize the need to study the effects of CAM in adult patients with pre-existing immunological memory and elderly patients with low immunological responses.

Nasopharyngeal-associated lymphoreticular tissue is known as the production site of nasal S-IgA, where IgA-committed B cells undergo class switching. Subsequently, IgA-committed B cells migrate to mucosal effector tissues including the nasal passages [26]. We reported recently that CAM enhances IgA class switching recombination through upregulation of BAFF in mucosal dendritic cells and activation-induced cytidine deaminase in B cells [14]. The present clinical results add support to these early studies.

Table 4. Rates of improvement of clinical symptoms after 5 days of no treatment and treatment with OSV, OSV+CAM, ZNV and ZNV+CAM.

Improvement (%)	Fever	Sore throat	Cough	Nasal discharge	Headache	Body aches
No treatment (n = 68)	94.1 (64/68)	92.0 (23/25)	35.4 (23/65)	41.5 (27/65)	96.0 (24/25)	100 (16/16)
OSV (n = 70)	94.3 (66/70)	68.2 (15/22)	31.3 (20/64)	39.4 (26/66)	100 (21/21)	100 (26/26)
OSV+CAM (n = 20)	95.0 (19/20)	80.0 (4/5)	58.8* (10/17)	61.1 (11/18)	100 (4/4)	100 (4/4)
ZNV (n = 27)	96.3 (26/27)	93.3 (14/15)	50.0 (12/24)	37.5 (9/24)	86.7 (13/15)	87.5 (7/8)
ZNV+CAM (n = 10)	100 (10/10)	100 (5/5)	60.0 (6/10)	77.8† (7/9)	100 (6/6)	100 (3/3)

Data are percentage of patients who reported disappearance of symptoms per patients with symptoms at the start of treatment.
*$P<0.05$, versus OSV (Fisher's exact test).
†$P<0.05$, versus ZNV (Fisher's exact test).
doi:10.1371/journal.pone.0070060.t004

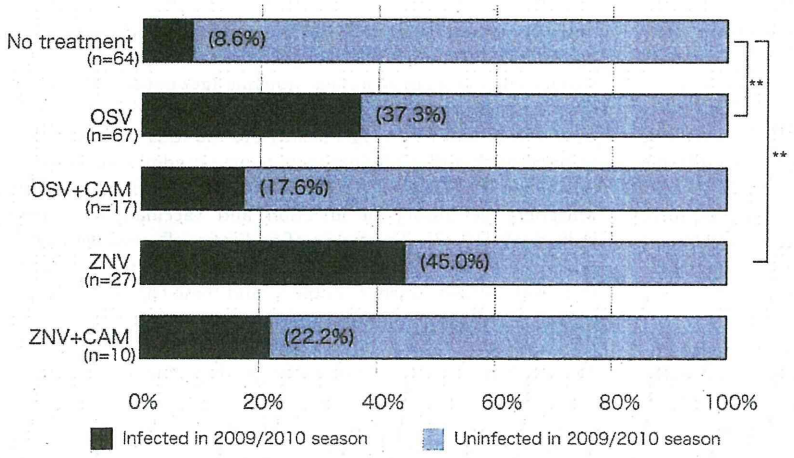

Figure 1. Re-infection rate in 2009/2010 season. The re-infection rate in 2009/2010 season in children who were infected with IAV during the 2008/2009 season and either untreated or treated with OSV, OSV+CAM, ZNV and ZNV+CAM. Data show the percentage of infected children in each group. *$P<0.05$, * *$P<0.01$, versus no treatment (Fisher's exact test with Bonferroni correction).
doi:10.1371/journal.pone.0070060.g001

In conclusion, the present study showed that CAM boosts and tends to restore the suppressed mucosal and/or systemic immunity in pediatric patients with influenza treated with OSV and ZNV.

Author Contributions

Conceived and designed the experiments: HK WS. Performed the experiments: MA NH YT SS KS TY KN MM MI YY SS. Analyzed the data: WS ET TS DM. Contributed reagents/materials/analysis tools: WS ET TS DM. Wrote the paper: HK WS.

References

1. Moscona A. (2005) Neuraminidase inhibitors for influenza. N Engl J Med 353:1363–1373.
2. Ison MG. (2011) Antivirals and resistance: influenza virus. Curr Opin Virol 1: 563 573.
3. Takahashi E, Kataoka K, Fujii K, Chida J, Mizuno D, et al. (2010) Attenuation of inducible respiratory immune responses by oseltamivir treatment in mice infected with influenza A virus. Microbes Infect 12:778 783.
4. Hashisaki GT. (1995) Update on macrolide antibiotics. Am J Otolaryngol 16:153–157.
5. Kudoh S, Uetake T, Hagiwara K, Hirayama M, Hus LH, et al. (1987) Clinical effects of low-dose long-term erythromycin chemotherapy on diffuse panbronchiolitis. Nihon Kyobu Shikkan Gakkai Zasshi 25:632 642.
6. Labro MT. (2001) Anti-inflammatory activity of macrolides: a new therapeutic potential? Antimicrob Agents Chemother 45:44–47.
7. Suzuki T, Yamada M, Sekizawa K, Hosoda M, Yamada N, et al. (2002) Erythromycin inhibits rhinovirus infection in cultured human tracheal epithelial cells. Am J Respir Crit Care Med 165:1113–1118.
8. Tahan F, Ozcan A, Koc N. (2007) Clarithromycin in the treatment of RSV bronchitis: a double-blind, randomized placebo-controlled trial. Eur Respir J 29:91–97.
9. Sato K, Suga M, Akaike T, Fujii S, Muranaka H, et al. (1998) Therapeutic effect of erythromycin of influenza virus-induced lung injury in mice. Am J Respir Crit Care Med 157:853 857.
10. Maeda S, Yamada Y, Nakamura H, Maeda T. (1999) Efficacy of antibiotics against influenza-like illness in an influenza epidemic. Pediatr Int 41:274–276.
11. Kido H, Okumura Y, Yamada H, Le TQ, Yano M. (2007) Protease essential for human influenza virus entry into cells and their inhibitors as potential therapeutic agents. Curr Pharm Des 13:405 414.
12. Tsurita M, Kurokawa M, Imakita M, Fukuda Y, Watanabe Y, et al. (2001) Early augmentation of interleukin (IL)-12 level in the airway of mice administrated orally with clarithromycin or intranasally with IL-12 results in alleviation of influenza infection. J Pharmacol Exp Ther 298:362–368.
13. Sawabuchi T, Suzuki S, Iwase K, Ito C, Mizuno D, et al. (2009) Boost of mucosal secretory immunoglobulin A response by clarithromycin in paediatric influenza. Respirology 14:1173 1179.
14. Takahashi E, Kataoka K, Indalao IL, Konoha K, Fujii K, et al. (2012) Oral clarithromycin enhances airway immunoglobulin A (IgA) immunity through induction of IgA class switching recombination and B-cell-activating factor of the tumor necrosis factor family molecule on mucosal dendritic cells in mice infected with influenza A virus. J Virol 86:10924–10934.
15. Infectious Disease Surveillance Center, National Institute of Infectious Diseases of Japan. (2009) 2008/09 influenza season, Japan. Infect Agents Surveill Rep 30:285 286. Available: http://idsc.nih.go.jp/iasr/30/357/tpc357.html. Accessed May 31. 2013.
16. Fujimoto C, Kido H, Sawabuchi T, Mizuno D, Hayama M, et al. (2009) Aspiration of nasal IgA secretion in normal subjects by nasal spray and aspiration. Auris Nasus Larynx 36:300–304.
17. Fujimoto C, Takeda N, Matsunaga A, Sawada A, Tanaka T, et al. (2012) Induction and maintenance of anti-influenza antigen-specific nasal secretory IgA levels and serum IgG levels after influenza infection in adults. Influenza Other Respi Viruses 6:396–403.
18. Holmgren J, Czerkinsky C. (2005) Mucosal immunity and vaccines. Nat Med 11:S45–53.
19. Doherty PC, Topham DJ, Tripp RA, Cardin RD, Brooks JW, et al. (1997) Effector $CD4^+$ and $CD8^+$ T-cell mechanisms in the control of respiratory virus infection. Immunol Rev 159:105 117.
20. Clements ML, Betts RF, Tierney EL, Murphy BR. (1986) Serum and nasal wash antibodies associated with resistance to experimental challenge with influenza A wild type virus. J Clin Microbiol 24:157 160.
21. Mizuno D, Ide-Kurihara M, Ichinomiya T, Kubo I, Kido H. (2006) Modified pulmonary surfactant is a potent adjuvant that stimulates the mucosal IgA production in response to the influenza virus antigen. J Immunol 176:1122–1130.
22. Nishino M, Mizuno D, Kimoto T, Shinahara W, Fukuta A, et al. (2009) Influenza vaccine with Surfacten, a modified pulmonary surfactant, induces systemic and mucosal immune responses without side effects in minipigs. Vaccine 27:5620–5627.
23. Murphy BR, Clements ML. (1989) The systemic and mucosal immune response of humans to influenza A virus. Curr Top Microbiol Immunol 146:107–116.
24. Liew FY, Russell SM, Appleyard G, Brand CM, Beale J. (1984) Cross-protection in mice infected with influenza A virus by the respiratory route is correlated with local IgA antibody rather than serum antibody or cytotoxic T cell reactivity. Eur J Immunol 14:350–356.
25. Renegar KB, Small PA Jr, Boykins LG, Wright PF. (2004) Role of IgA versus IgG in the control of influenza viral infection in the murine respiratory tract. J Immunol 173:1978–1986.
26. Kunkel EJ, Butcher EC. (2003) Plasma-cell homing. Nat Rev Immunol 3:822–829.

OPEN ACCESS Freely available online

PLOS ONE

Anti-Influenza Activity of C_{60} Fullerene Derivatives

Masaki Shoji[1], Etsuhisa Takahashi[2], Dai Hatakeyama[1], Yuma Iwai[1], Yuka Morita[1], Riku Shirayama[1], Noriko Echigo[1], Hiroshi Kido[2], Shigeo Nakamura[3], Tadahiko Mashino[4], Takeshi Okutani[1], Takashi Kuzuhara[1]*

1 Laboratory of Biochemistry, Faculty of Pharmaceutical Sciences, Tokushima Bunri University, Yamashiro-cho, Tokushima, Japan, **2** Division of Enzyme Chemistry, Institute for Enzyme Research, The University of Tokushima, Tokushima, Japan, **3** Department of Chemistry, Nippon Medical School, Nakahara-ku, Kawasaki, Kanagawa, Japan, **4** Department of Pharmaceutical Sciences, Faculty of Pharmacy, Keio University, Minato-ku, Tokyo, Japan

Abstract

The H1N1 influenza A virus, which originated in swine, caused a global pandemic in 2009, and the highly pathogenic H5N1 avian influenza virus has also caused epidemics in Southeast Asia in recent years. Thus, the threat from influenza A remains a serious global health issue, and novel drugs that target these viruses are highly desirable. Influenza A RNA polymerase consists of the PA, PB1, and PB2 subunits, and the N-terminal domain of the PA subunit demonstrates endonuclease activity. Fullerene (C_{60}) is a unique carbon molecule that forms a sphere. To identify potential new anti-influenza compounds, we screened 12 fullerene derivatives using an *in vitro* PA endonuclease inhibition assay. We identified 8 fullerene derivatives that inhibited the endonuclease activity of the PA N-terminal domain or full-length PA protein *in vitro*. We also performed *in silico* docking simulation analysis of the C_{60} fullerene and PA endonuclease, which suggested that fullerenes can bind to the active pocket of PA endonuclease. In a cell culture system, we found that several fullerene derivatives inhibit influenza A viral infection and the expression of influenza A nucleoprotein and nonstructural protein 1. These results indicate that fullerene derivatives are possible candidates for the development of novel anti-influenza drugs.

Citation: Shoji M, Takahashi E, Hatakeyama D, Iwai Y, Morita Y, et al. (2013) Anti-Influenza Activity of C_{60} Fullerene Derivatives. PLoS ONE 8(6): e66337. doi:10.1371/journal.pone.0066337

Editor: Paul Digard, University of Edinburgh, United Kingdom

Received January 10, 2013; **Accepted** May 3, 2013; **Published** June 13, 2013

Funding: This study was supported by the Japan Society for the Promotion of Science (grant no. 20890273, 22590422, 22790098, and 23780051). The funders had no role in study design, data collection and analysis, decision to publish, or preparation of the manuscript.

Competing Interests: The authors have declared that no competing interests exist.

* E-mail: kuzuhara@ph.bunri-u.ac.jp

Introduction

In 1918, an influenza A pandemic caused 50 million deaths worldwide [1], and the development of strategies that can be used to prevent future expansions of this virus continues to be an important endeavor [2]. The avian H5N1 influenza A virus is highly pathogenic to humans [3], and the emergence of a new strain of this virus in 2009, the swine-originating A/H1N1 pdm influenza virus, further emphasizes that this issue is a serious global health problem [4,5]. Although inhibitors of influenza A, e.g., the neuraminidase-like compound oseltamivir, are widely used as antiviral drugs [6,7], the adverse effects of these agents and the emergence of viral strains that are resistant to these drugs have now been reported [8,9].

To prevent and control influenza outbreaks, the development of novel antiviral drugs that are not based on neuraminidase inhibition is now regarded as critical. The influenza A genome consists of segmented single-stranded RNA (-), and its transcription and replication require the activity of a highly conserved RNA-dependent RNA polymerase [10,11]. This polymerase is essential for the propagation of the influenza A virus and is a very promising target for the development of antiviral drugs. The influenza A virus RNA polymerase is composed of three subunits–PA, PB1, and PB2 [12]–and synthesizes viral mRNA using short capped primers that are cleaved from the host's cellular pre-mRNAs by the viral endonuclease [13,14]. Yuan et al. and Dias et al. have shown that the N-terminal domain of the PA subunit contains the active site of the endonuclease, and that this domain also harbors RNA/DNA endonuclease activity [13,14]. Hence, we speculate that PA endonuclease would contain very effective targets for the development of novel anti-influenza A drugs, as we have shown that several chemicals, e.g., catechins, phenethylphenyl phthalimide analogs, and marchantin analogs, inhibit this endonuclease and possess antiviral activity [15–17].

Fullerene (C_{60}), a carbon buckyball, was discovered by Harold Kroto, James R. Heath, Sean O'Brien, Robert Curl, and Richard Smalley in 1985 [18]. It has since been utilized in electronic and mechanical applications [19]. In physiological studies, the biological effects of water-soluble fullerene derivatives containing several hydrophilic groups are noteworthy because fullerene itself is water-insoluble. Water-soluble fullerene derivatives are known to possess various biological and pharmacological properties, including antioxidant activity and inhibitory effects against human immunodeficiency virus (HIV) proteases and DNA photocleavage [20–23]. Mashino et al. also demonstrated that pyrrolidinium fullerene derivative 6 (Fig. 1) has antiproliferative and antibacterial activity [24], malonic acid fullerene derivative 2 (Fig. 1) has excellent antioxidant activity [25], and proline-modified fullerene derivative 3 (Fig. 1) inhibits HIV-reverse transcriptase [22]. Thus, fullerene derivatives are expected to become a novel type of medication because of their unique skeleton.

In our current study, we used an *in vitro* influenza PA endonuclease assay to analyze the effects of 12 different fullerene derivatives on the endonuclease activity of the PA N-terminal

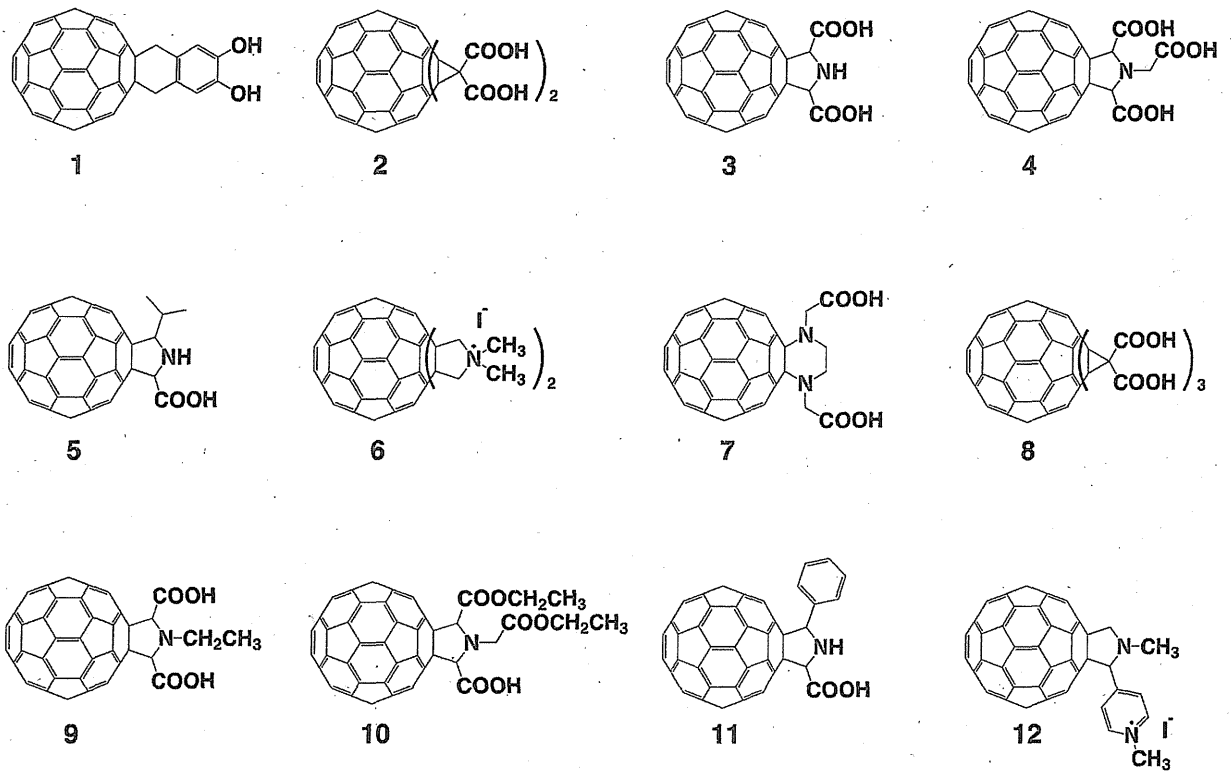

Figure 1. Chemical structures of the C60 fullerene derivatives tested in this study. The chemical structures of the fullerene derivatives examined in this study are shown. The sources for these structures are described in the Materials and Methods. No. 1, 1,4-dihydro-6,7-dihydroxy [60]fullerenonaphthlene; no. 2, [60]fullerenodicyclopropane-1,1,1′,1′-tetracarboxylic acid; no. 3: [60]fullerenopyrrolidine-2,5-dicarboxylic acid; no. 4, 1-carboxymethyl [60]fullerenopyrrolidine-2,5-dicarboxylic acid; no. 5, 5-isopropyl [60]fullerenopyrrolidine-2-carboxylic acid; no. 6:1,1,1′,1′-tetramethyl [60]fullerenodipyrrolidinium diiodide; no. 7, [60]fullerenopiperazine-1,4-diacetic acid; no. 8: [60]fullerenotricyclopropane-1,1,1′,1′,1′′,1′′-hexacarboxylic acid; no. 9, 1-ethyl [60]fullerenopyrrolidine-2,5-dicarboxylic acid; no. 10, 1-ethoxycarbonylmethyl [60]fullerenopyrrolidine-2,5-dicarboxylic acid 2-ethyl ester; no. 11, 5-phenyl [60]fullerenopyrrolidine-2-carboxylic acid; and no. 12, 4-(1′-methyl [60]fullerenopyrrolidin-2′-yl)-1-methylpyridinium iodide.
doi:10.1371/journal.pone.0066337.g001

domain and full-length PA. We found that the fullerene derivatives inhibit influenza PA endonuclease activity and viral infection. Our results indicate the possibility of developing fullerene derivatives into novel anti-influenza A drugs in the future.

Results

Inhibition of PA Endonuclease by Fullerene Derivatives

For the *in vitro* PA endonuclease assay, we expressed and purified a recombinant influenza PA endonuclease domain (1–220 residues; Fig. 2A, B) using bacteria as described previously [15–17]. For the assay, we incubated 0.1 μM recombinant PA endonuclease domain with 1 or 10 μM of each fullerene derivative (Fig. 2C). The PA endonuclease domain digested M13 mp18 circular single-stranded DNA *in vitro* (Fig. 2C, lanes 1 and 2) [12–16], and we investigated whether any of the fullerene derivatives could inhibit this activity. The fullerene derivatives 2–5, 7, 8, 10, and 11 significantly inhibited the digestion of M13 mp18 at a dose of 10 μM, no. 12 slightly inhibited digestion, and no. 1, 6, and 9 had no or weak inhibitory activity (Fig. 2C). This is the first study to report that fullerene derivatives can inhibit the activity of influenza enzymes. Fullerene derivative no. 6 caused a mobility shift of M13 mp18, possibly because it has a cationic amine group (Fig. 2C, lane 13). The solubility of the fullerene derivatives 1 and 6 in water was relatively low, which might have been the cause of their decreased activity levels.

To investigate the effects of full-length PA protein on PA endonuclease activity and the inhibitory activity of the fullerene derivatives, we examined whether the fullerene derivatives also inhibit the endonuclease activity of full-length PA protein. We expressed the recombinant full-length PA protein by using a baculovirus to infect Sf9 insect cells (Fig. 3A) and purified it using a Ni-agarose and HiTrap-Q column (Fig. 3B). The recombinant full-length PA protein demonstrated endonuclease activity (Fig. 3C, lanes 1 and 2) [26,27]. Then, we tested the 12 fullerene derivatives using this same assay. The fullerene derivatives 2–5, 7, 8, 10, and 11 inhibited the endonuclease activity of full-length PA (Fig. 3C), which is consistent with the results for the PA endonuclease domain (Fig. 2C). The M13 mp18 band in the no. 12-treated lane was degraded (Fig. 3C lane 14), the band in the no. 1 and 9-treated lanes slightly remained (Fig. 3C, lanes 3 and 11), suggesting that fullerene derivatives no. 1 and 9 also slightly inhibited the PA endonuclease activity of the full length PA protein.

As shown in Figs. 2C and 3C, the M13 mp18 band in the no. 6-treated lanes shifted and was clear (Fig. 3C lane 8), respectively, suggesting that no. 6 has the ability to cleave DNA. Thus, we examined the nuclease activity of the fullerene derivatives (Fig. 4). The result showed that fullerene derivative no. 6 by itself has

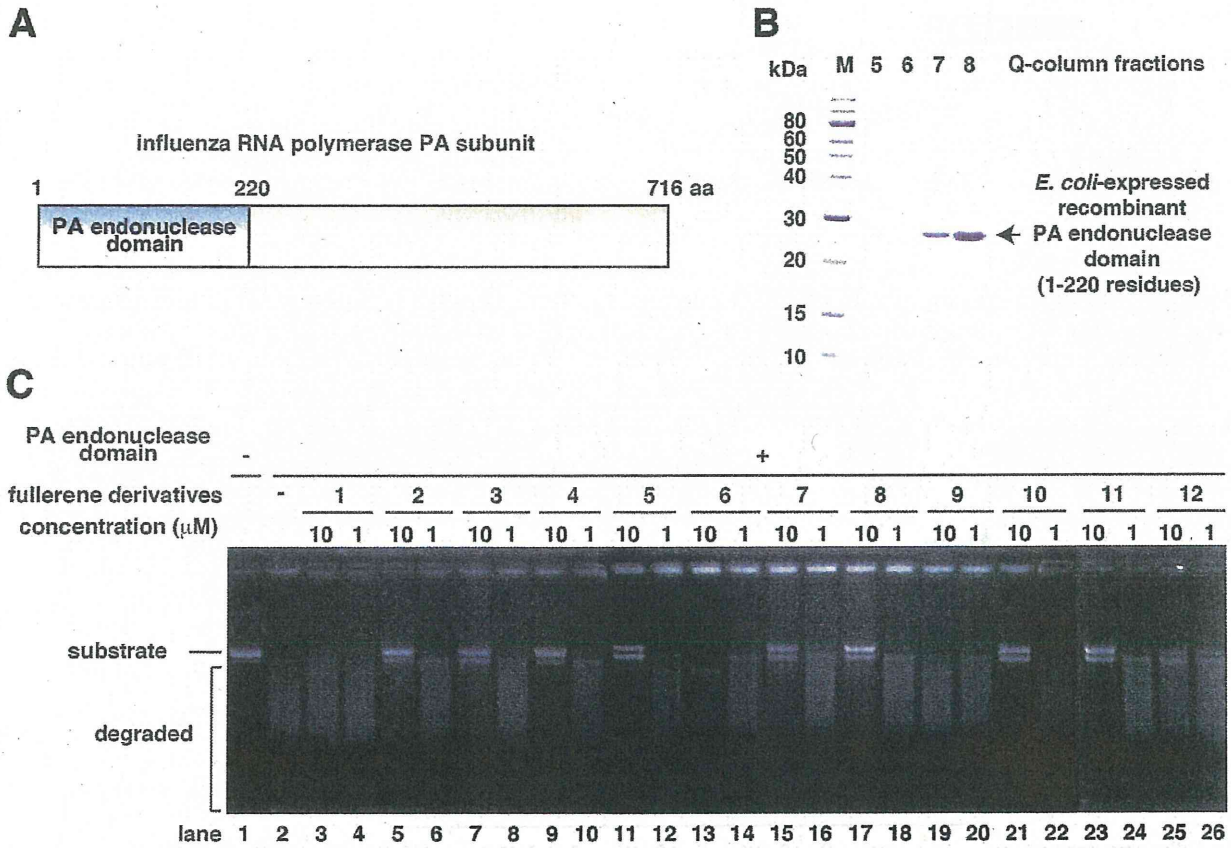

Figure 2. Inhibition of the activity of the PA endonuclease domain by the fullerene derivatives. (**A**) Schematic of the PA subunit of influenza RNA polymerase. (**B**) Purification of the bacterially expressed PA endonuclease domain using a HiTrap-Q column. The arrow indicates the PA endonuclease domain. (**C**) The effects of the various fullerene derivatives on the endonuclease activity of the PA N-terminal domain of the influenza A RNA polymerase were tested. The recombinant PA N-terminal domain protein was added to each reaction at a concentration of 0.25 μg/100 μL. A zero control (i.e., no PA domain added) was also assayed. The fullerene derivatives were added at a dose of 1 or 10 μM, and M13 mp18 was used as the substrate.
doi:10.1371/journal.pone.0066337.g002

significant nuclease activity in the absence of PA endonuclease (Fig. 4). No. 12 also showed weaker nuclease activity by itself (Fig. 4).

Docking Simulation of Influenza A Endonuclease and C_{60} Fullerene

Previously, we reported that 3 of 34 phthalimide chemicals and 5 of 33 phytochemicals inhibited PA endonuclease activity [12,15,16]. In the case of the fullerenes, 8 of the 12 fullerene derivatives inhibited PA endonuclease activity; thus, we thought that the fullerene skeleton itself could fit into the active pocket of the influenza PA endonuclease domain. To investigate how the fullerene molecule binds to and fits in the active pocket of the PA endonuclease domain, we performed *in silico* docking simulation analysis of this interaction at the level of the tertiary structure using Molecular Operating Environment software (MOE; Chemical Computing Group, Quebec, Canada) [28]. The results show that fullerene fits into and fills the active pocket of the endonuclease domain of the influenza RNA polymerase (Fig. 5A), suggesting that this may be the major cause of the inhibitory mechanism. The two divalent ions of manganese in the active pocket are reportedly necessary for influenza endonuclease activity [13,14]. Fullerene binds to manganese ions by arene-cation interactions at the back of the active pocket (Fig. 5B and 5C), suggesting that this binding is also one of the inhibitory mechanisms.

Toxicity of the Fullerene Derivatives Against the Madin-Darby Canine Kidney Cell Line

We evaluated the toxicity of the fullerene derivatives against Madin-Darby canine kidney (MDCK) cells before examining their antiviral activity against the influenza A virus. Various concentrations (12.5–100 μM) of the fullerene derivatives were added to cultures of MDCK cells. Marchantin E (ME) was used as the positive controls for anti-influenza activity [16]. At 24 h post-incubation, the cell viability of the treated-cells was determined using an MTT cell proliferation assay (Fig. 6A). The viability of the cells treated with the fullerene derivatives 1–12 and ME was not significantly different to that of the cells treated with dimethyl sulfoxide (DMSO) at a concentration of 12.5 to 100 μM. We also performed naphthol blue black assay for cytotoxicity of fullerene derivatives (Fig. 6B). At 24 h post-incubation, the viable cells were stained using a blue dye. The wells treated with 0.8–100 μM of the fullerene derivatives 1–12 and DMSO were stained blue (Fig. 6B). Taken together, these data show that the fullerene derivatives (1–12) are not toxic to MDCK cells up to a concentration of 100 μM.

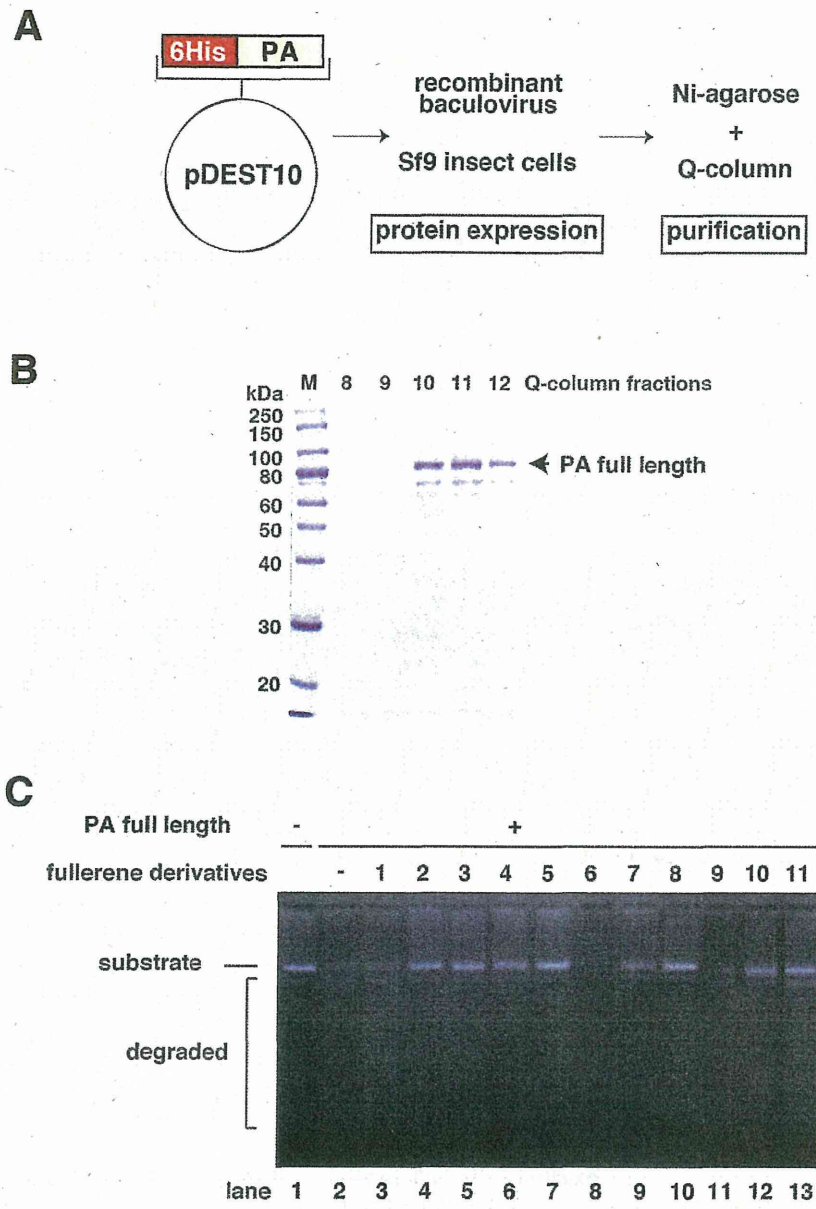

Figure 3. Inhibition of the activity of full-length PA endonuclease by the fullerene derivatives. (**A**) Schematic of the constructed plasmid, baculovirus expression, and purification of full-length PA protein. (**B**) Purification of full-length PA protein using a HiTrap-Q column. The numbers indicate the fractions. The arrow indicates full-length PA protein. (**C**) The effects of the various fullerene derivatives on the endonuclease activity of full-length PA protein of influenza A RNA polymerase were tested. Recombinant full-length PA protein was added to each reaction at a concentration of 0.25 μg/100 μL. A zero control (i.e., no PA protein added) was also assayed. The fullerene derivatives were added at a dose of 10 μM and M13 mp18 was used as the substrate.
doi:10.1371/journal.pone.0066337.g003

Inhibition of Influenza A Virus Infection by the Fullerene Derivatives

We evaluated the antiviral activity of the fullerene derivatives against the influenza A virus (A/Puerto Rico (PR)/8/34 (H1N1) or A/Aichi/2/68 (H3N2)). Various concentrations of the fullerene derivatives and the virus were mixed and added to cultures of MDCK cells [29]. ME and DMSO were used as positive and negative controls for the inhibitory effect of influenza A virus infection, respectively. At 24 h post-infection, we performed influenza A nucleoprotein (NP)-immunostaining of the treated cells, and the stained cells were counted. At 100 μM, fullerene derivatives no. 2–8, 11 and 12 significantly reduced the number of NP-positive cells in comparison with the control (DMSO), in A/PR8/34 (H1N1)-infected cells (Fig. 7A & C). Also in A/Aichi/2/68 (H3N2)-infected cells, at 100 μM, fullerene derivatives no. 2–8 and 10–12 significantly reduced the number of NP-positive cells in comparison with the DMSO (Fig. 7B & D). The fullerene derivatives 10 in A/PR8/34 (H1N1) also slightly decreased the

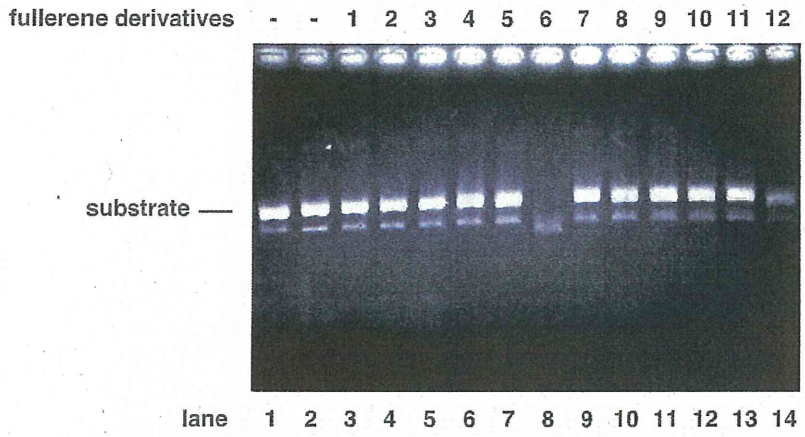

Figure 4. Nuclease activity of the fullerene derivatives. The method was the essentially same as that of Figs. 2 & 3, except the condition of the absence of PA protein. The fullerene derivatives were added at a dose of 10 μM and M13 mp18 was used as the substrate. The digestion of the substrate was examined by agarose electrophoresis.
doi:10.1371/journal.pone.0066337.g004

number of NP-positive cells (Fig. 7A & C). Conversely, the number of NP-positive cells treated with the fullerene derivatives 1 and 9 were comparable to that of the DMSO-treated cells (Fig. 7A–D).

Based on these results, to compare their activities quantitatively, we calculated IC_{50} values of fullerene derivatives against A/PR8/34 (H1N1) and A/Aichi/2/68 (H3N2) strains. Against H1N1 PR8 strain, IC_{50} values are as follows: 57 μM for fullerene derivatives no. 2; 70 μM for no. 4; 37 μM for no. 5; 20 μM for no. 6; 37 μM for no. 8; 44 μM for no. 11; 78 μM for no. 12; more than 100 μM for no. 3, 7 or 10; 43 μM for ME (Table 1). Against H3N2 Aichi strain, IC_{50} values: 91 μM for fullerene derivatives no. 4; 31 μM for no. 6; 63 μM for no. 12; more than 100 μM for no. 2, 3, 5, 7, 8, 10 or 11; 53 μM for ME (Table 1). IC_{50} values of fullerene derivatives no. 1 or 9 could not be calculated against the strains because of their weak activities (Table 1). Taken together, it indicated that several fullerene derivatives have stronger anti-influenza activity than ME.

Moreover, we examined the expression levels of viral proteins by western blotting of treated-cell lysates in A/PR8/34 (H1N1)-infected wells at 4, 8, 12 (Fig. 8A), and 24 h (Fig. 8B) post-infection. The expression levels of influenza A NP and nonstructural protein 1 (NS1) proteins in the cells treated with the fullerene derivatives 5, 6, and 11, and ME were reduced as compared with that of the DMSO-treated cells, but slightly reduced in the wells

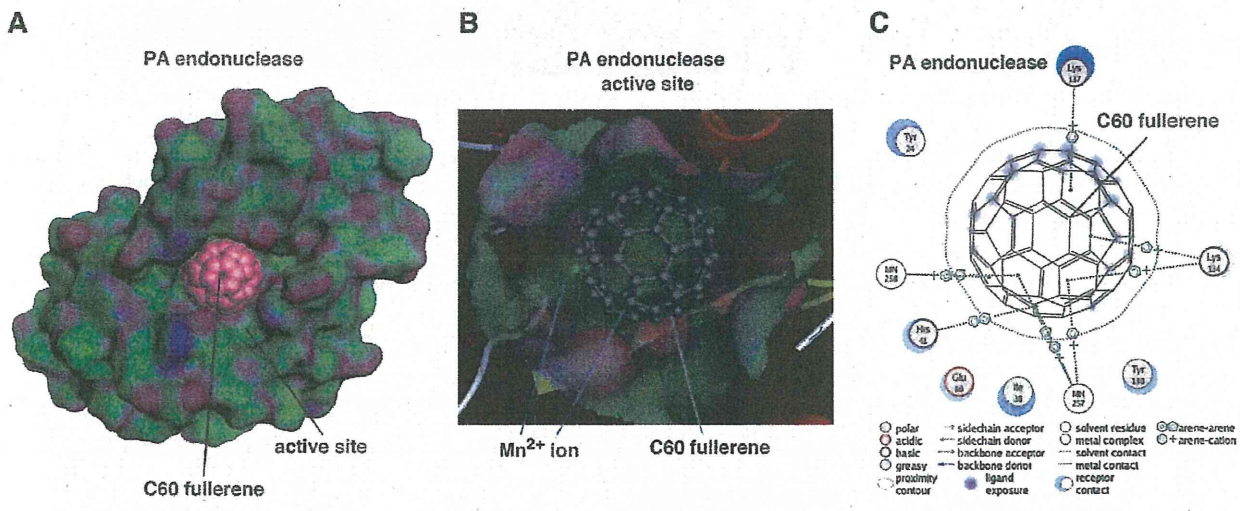

Figure 5. Docking simulation of C_{60} fullerene with influenza PA endonuclease. (**A**) Docking simulation analysis of C_{60} fullerene with the PA endonuclease domain of influenza A RNA polymerase. The fullerene is shown as a sphere. The surface of the pocket of PA endonuclease is shown in green and purple. The pink ball indicates the carbon atoms in the fullerene. (**B**) The fitting of the fullerene to the active pocket of PA endonuclease. PA endonuclease is depicted as a ribbon structure. The α-helix and β-strands are shown in red and yellow, respectively. The fullerene is shown as a gray stick structure. The manganese ions in PA endonuclease are behind the fullerene. (**C**) Two-dimensional analysis of the interactions between fullerene and PA endonuclease. The fullerene is shown in the center with the key and with the interacting amino acids shown around it. MN indicates the Mn^{2+} ions. The modes of interaction are shown at the bottom. The arene of the fullerene interacts with 2 Mn^{2+} ions and the amino acids, e.g., lysine and histidine, in PA endonuclease.
doi:10.1371/journal.pone.0066337.g005

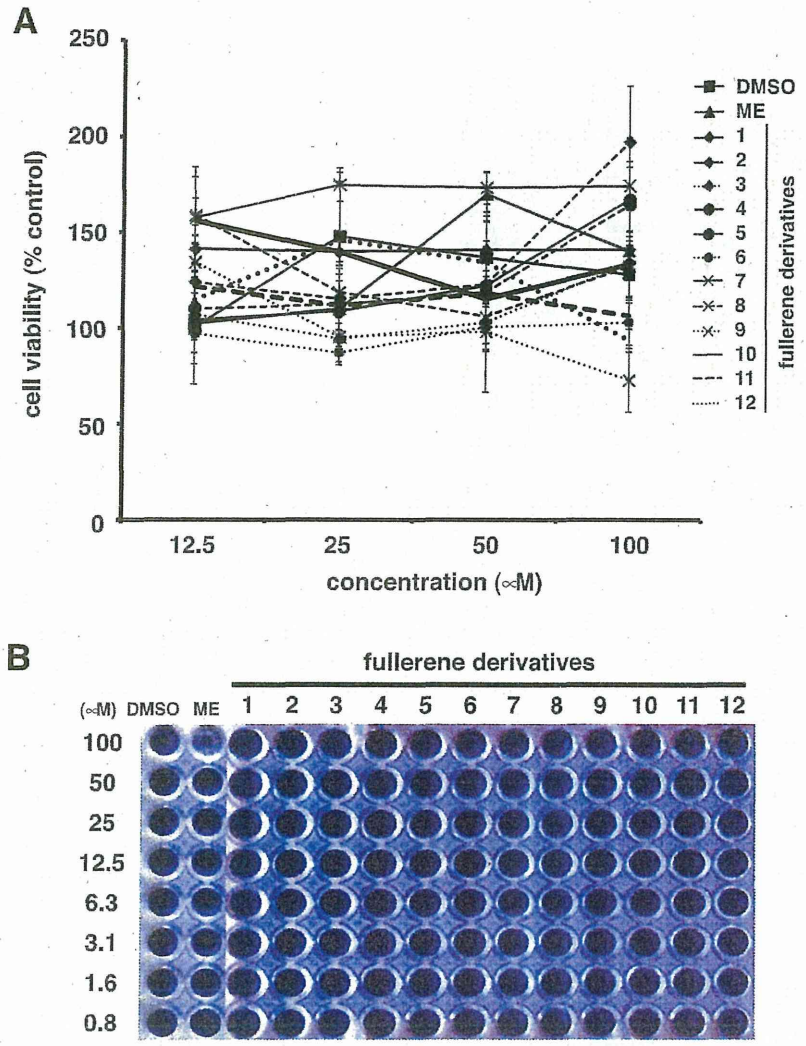

Figure 6. Toxicity of the fullerene derivatives against MDCK cells. (**A**) Various concentrations (12.5–100 μM) of the fullerene derivatives (n = 4) were added to cultures of MDCK cells. DMSO and ME were used as negative and positive controls for anti-influenza activity, respectively. At 24 h post-incubation, cell viability was determined using an MTT cell proliferation assay. Data represent the mean ± standard error of the mean (S.E.M.). (**B**) Various concentrations (0.8–100 μM) of the fullerene derivatives were added to cultures of MDCK cells. ME was used as positive control for cytotoxicity. At 24 h post-incubation, the cells were fixed and viable cells were stained with a naphthol blue black solution.
doi:10.1371/journal.pone.0066337.g006

treated with the fullerene derivatives 2–5, 7, 8, 10 and 12 (Fig. 8A and 8B). Conversely, the expression levels of influenza A NP and NS1 proteins in cells treated with the fullerene derivatives 1 and 9 were comparable to those in the DMSO-treated cells (Fig. 8A and 8B). Taken together, these data show that the fullerene derivatives 2–8 and 10–12 possess antiviral effects against the influenza A virus, and their mechanism of action may be by the inhibition of PA endonuclease activity (no. 2–5, 7, 8, and 11) or their ability to cleave viral RNA (no. 6 and 12).

Discussion

In this study, we showed that the fullerene derivatives 2–5, 7, 8, 10, and 11 or 6 and 12 possess inhibitory activity against influenza PA endonuclease or the ability to cleave DNA, respectively. Moreover, we showed that the fullerene derivatives 2–8 and 10–12 inhibit the infection of the influenza A virus. Above all, no. 6 showed the strongest antiviral activity. A previous report showed that certain fullerene derivatives have DNA and RNA cleavage activity [20,30]. As shown in Figs. 2C and 3C, the M13 mp18 band in the no. 6-treated lanes shifted and was clear, respectively. Since no. 6 has the activity to cleave DNA, the antiviral activity of no. 6 may be caused by its cleavage of viral RNA. Therefore, fullerene derivatives are promising novel anti-influenza chemicals. These data are an important advance that could be used in future strategies to refine fullerene-based drug designs. Our analysis provides valuable new information for the design of novel anti-influenza drugs. There was no correlation between the PA endonuclease and antiviral activity of fullerene derivative no. 12. This may be because it targets influenza A virus attachment/entry or growth in cells and also because of differences in its permeability into the cells. When we performed the anti-viral experiment without pre-incubation, we could not find an

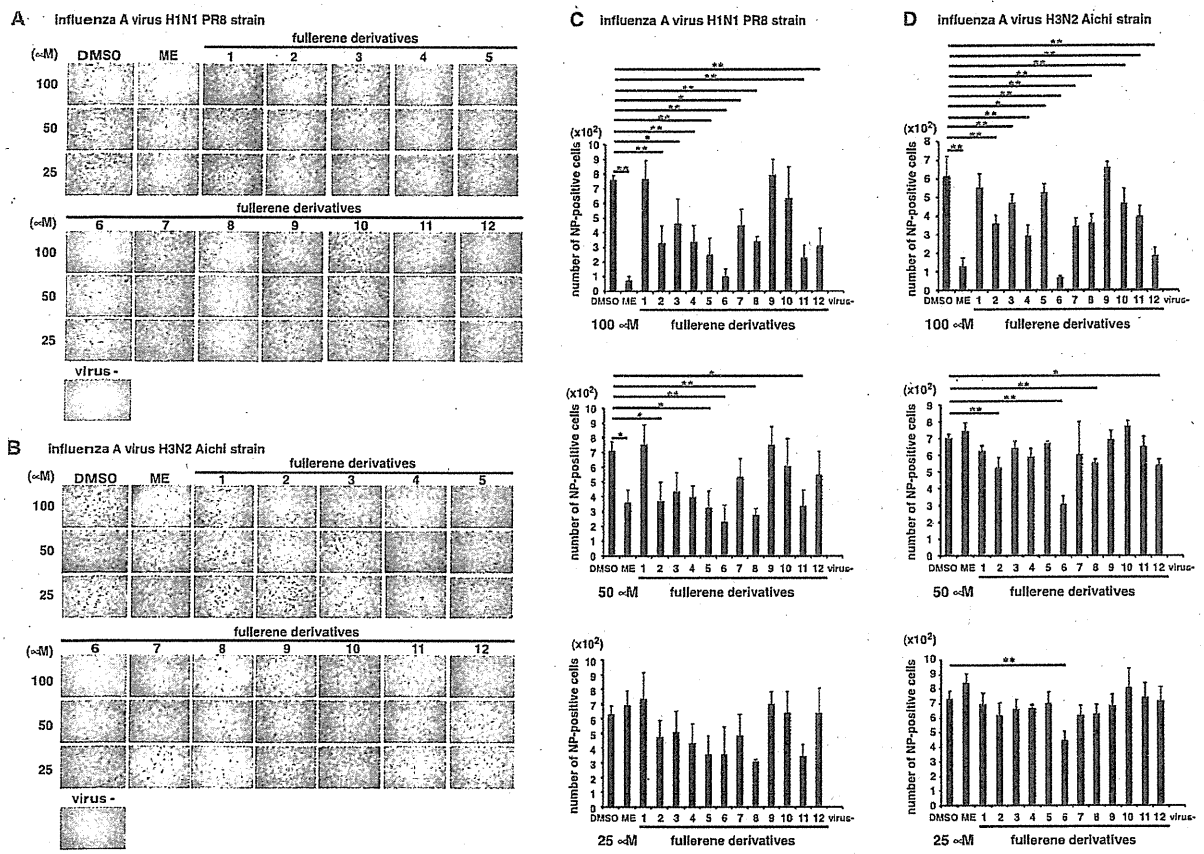

Figure 7. Immunostaining of influenza A virus-infected cells. Various concentrations of the fullerene derivatives (25–100 μM) and an MOI of 1 influenza A virus (A/PR/8/34 (H1N1) (n = 3) (**A and C**) or A/Aichi (H3N2) (n = 4) (**B and D**)) were mixed and added to cultures of MDCK cells. At 24 h post-infection, influenza A NP-immunostaining of the treated cells was performed. The wells were photographed under a microscope (×4) (**A and B**), and the stained cells were counted (**C and D**). DMSO (n = 4) and ME (n = 4) were used as negative and positive controls for the inhibitory effect of influenza A virus infection, respectively. Data represent the mean ± S.E.M. $*p<0.05$, $**p<0.01$.
doi:10.1371/journal.pone.0066337.g007

experimental condition under which the fullerene derivatives showed anti-virus activity. This suggests that the fullerene derivatives may have virucidal activity or they may enter cells by associating with the virus.

Other groups also have reported novel anti-influenza polymerase inhibitors such as T-705 and L-742,001 [27,31–36], which are substituted pyrazine and piperidine compounds, respectively. Since the chemical structures of fullerene derivatives are completely different from those of them, indicating that fullerene derivatives are quite novel anti-influenza compounds.

Finally, we conclude that the chemical and biochemical information presented here will be very useful for the future development of novel fullerene-based drugs against influenza A.

Materials and Methods

Preparation of the C_{60} Fullerene Derivatives

Water-soluble fullerene derivatives were synthesized and purified using previously reported methods with small modifications [20–25]. All of the fullerene derivatives were dissolved in DMSO to a concentration of 10 mM as stock solutions. The fullerene derivatives (Fig. 1) used in these experiments consisted of the following [20–25]: no. 1, 1,4-dihydro-6,7-dihydroxy [60]fullerenonaphthlene; no. 2, [60]fullerenodicyclopropane-1,1,1′,1′-tetracarboxylic acid; no. 3, [60]fullerenopyrrolidine-2,5-dicarboxylic acid; no. 4, 1-carboxymethyl [60]fullerenopyrrolidine-2,5-dicarboxylic acid; no. 5, 5-isopropyl [60]fullerenopyrrolidine-2-carboxylic acid; no. 6, 1,1,1′,1′-tetramethyl [60]fullerenodipyrrolidinium diiodide; no. 7, [60]fullerenopiperazine-1,4-diacetic acid; no. 8, [60]fullerenotricyclopropane-1,1,1′,1′,1″,1″-hexacarboxylic acid; no. 9, 1-ethyl [60]fullerenopyrrolidine-2,5-dicarboxylic acid; no. 10, 1-ethoxycarbonylmethyl [60]fullerenopyrrolidine-2,5-dicarboxylic acid 2-ethyl ester; no. 11, 5-phenyl [60]fullerenopyrrolidine-2-carboxylic acid; and no. 12, 4-(1′-methyl [60]fullerenopyrrolidin-2′-yl)-1-methylpyridinium iodide.

Bacterial Expression and Purification of the PA Endonuclease Domain

The influenza A virus (A/PR/8/34 (H1N1)) RNA polymerase PA plasmid, pBMSA-PA, was obtained from the DNA bank at Riken BioResource Center (Tsukuba, Japan; originally deposited by Susumu Nakada) [37]. The cDNA fragment corresponding to the PA N-terminal endonuclease domain (residues 1–220; Fig. 2A) was amplified by polymerase chain reaction (PCR) [38] from pBMSA-PA. The amplified product was subcloned into the pET28a (+) plasmid (Novagen, Madison, WI, USA). The induction of recombinant protein expression was achieved by the addition of isopropyl-D-thiogalactopyranoside [39], and this

Table 1. IC_{50} of the fullerene derivatives against influenza A virus H1N1 and H3N2 strains.

		IC_{50} (μM)	
		H1N1 PR8 strain	H3N2 Aichi strain
Marchantin E		43	53
Fullerene derivatives	no. 1	ND	ND
	no. 2	57	>100
	no. 3	>100	>100
	no. 4	70	91
	no. 5	37	>100
	no. 6	20	31
	no. 7	>100	>100
	no. 8	37	>100
	no. 9	ND	ND
	no. 10	>100	>100
	no. 11	44	>100
	no. 12	78	63

ND: not detected.
doi:10.1371/journal.pone.0066337.t001

was followed by purification using Ni^{2+}-agarose [40]. The recombinant PA endonuclease domain protein was further purified to near homogeneity (Fig. 2B) using a HiTrapQ-FF column (GE Healthcare, Buckinghamshire, UK).

Baculoviral Expression and Purification of the Full-length PA Subunit

The cDNA fragment corresponding to the full-length protein-coding region of PA was amplified by PCR [38] from pBMSA-PA using the primers PA_start_TOPO (CAC CAT GGA AGA TTT TGT GCG AC), PA stop (CTA ACT CAA TGC ATG TGT AAG), PA_mid_anti (TCT TTG GAC ATT TGA GAC AG), and PA_mid_TOPO (CAC CAA TTG AAG AAA GGT TTG). The amplified product was then subcloned into the pENTR/D-TOPO plasmid (Gateway®, Life Technologies™, Carlsbad, CA, USA) using topoisomerase I cloning. The resulting construct was then converted to pDEST10-PA using the clonase (Fig. 3A). The plasmid was transfected into Sf9 insect cells using the helper virus. The resultant baculovirus was again transfected into Sf9 cells [41]. The expressed full-length PA protein was purified using Ni^{2+}-agarose and a HiTrap Q FF column (GE Healthcare) with the AKTA prime plus system (Fig. 3B).

PA Endonuclease Activity and Fullerene Derivatives Nuclease Assays

Influenza A RNA polymerase PA endonuclease activity assays were performed as described by Dias et al. with some modifications [12–16]. Briefly, the pH was lowered from 8.0 to 7.3, and 1 μg M13 mp18 single-stranded circular phage DNA was used as the substrate. A total of 0.25 μg recombinant PA endonuclease domain or full-length PA protein were added to 100 μL assay buffer for each reaction (the final concentration of the protein was approximately 0.1 μM). For the fullerene derivative nuclease assay, no PA protein was added at this step. The fullerene derivatives (summarized in Fig. 1) were then added to the reaction, and the products were analyzed by agarose electrophoresis and stained with ethidium bromide.

In Silico Docking Simulation Analysis of Fullerene C_{60} and the PA Endonuclease Domain of Influenza RNA Polymerase

All molecular modeling studies were performed using MOE software (Chemical Computing Group) [26,42,43]. Information regarding the tertiary structure of the influenza PA endonuclease domain (PDB ID: 3HW6) was obtained from a protein data bank [29]. This enzyme was prepared for docking studies in which (1)

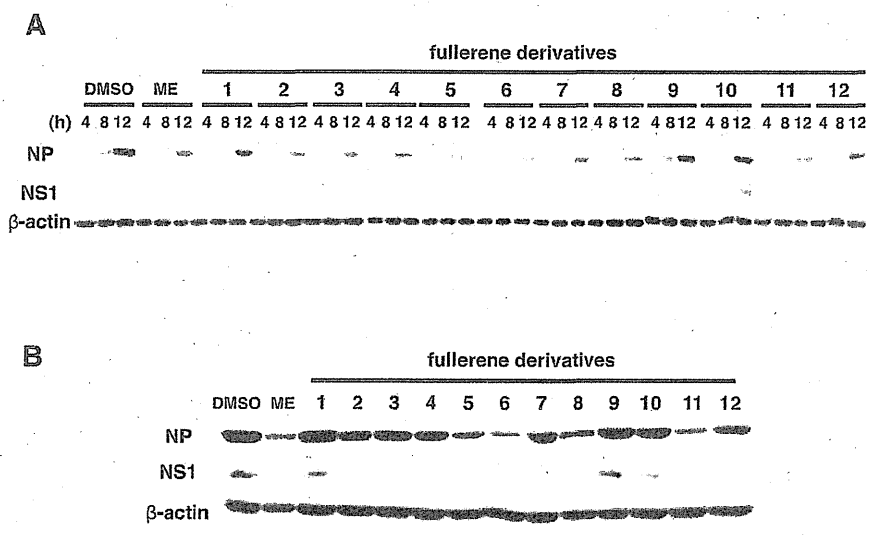

Figure 8. Expression levels of influenza A viral proteins. We mixed 100 μM of the fullerene derivatives or ME and an MOI of 1 influenza A virus (A/PR/8/34 (H1N1)) and added the mixture to cultures of MDCK cells. At 4, 8, 12 (**A**), and 24 h (**B**) postinfection, the expression levels of influenza A NP and NS1 proteins in treated-cell lysates were analyzed by western blotting, and β-actin was analyzed as an internal control. The experiments were performed three times and the results were reproducible.
doi:10.1371/journal.pone.0066337.g008

the ligand molecule was removed from the active site of the enzyme; (2) hydrogen atoms were added to the structure using standard geometry; (3) the structure was minimized using an MMFF94s force-field; (4) MOE Alpha Site Finder was used to search for active sites within the enzyme structure and dummy atoms were created from the obtained alpha spheres; and (5) the obtained model was then used in the Dock program (Ryoka Systems Inc., Tokyo, Japan). The conformation of the fullerene was generated by systematic, stochastic searches and Low Mode MD (molecular dynamics).

MTT Cell Proliferation Assay

The cytotoxicity of the fullerene derivatives in MDCK cells was determined with an MTT cell proliferation assay kit according to the manufacturer's instructions (Cayman, Arbor, MI, USA). Briefly, MDCK cells were cultured in Dulbecco's modified Eagle medium (DMEM; Gibco/Invitrogen, Carlsbad, CA, USA) supplemented with 10% fetal bovine serum, 1% penicillin-streptomycin, and 4 mM L-glutamine at 37°C under 5% CO_2. A confluent monolayer of MDCK cells was prepared in each well of a 96-well plate. Various concentrations (12.5–100 μM) of the fullerene derivatives and ME in DMSO (100 μM chemicals: 1%, 50 μM: 0.5%, 25 μM: 0.25%, 12.5 μM: 0.125%.), which were used as the anti-influenza activity [16], were mixed in an infection medium (DMEM supplemented with 1% bovine serum albumin, 1% penicillin-streptomycin, and 4 mM L-glutamine). The mixture was added to the cells, and the treated cells were incubated for 24 h at 37°C under 5% CO_2. After incubation, the cells were treated with the MTT reagent and incubated for 4 h at 37°C under 5% CO_2. The wells were treated with the crystal dissolving solution to lyse the formazan produced in the cells, and the absorbance of each well was measured at 570 nm using a microplate reader.

Cytotoxicity Assay by Naphthol Blue Black

A confluent monolayer of MDCK cells was prepared in each well of a 96-well plate. Various concentrations (0.8–100 μM) of the fullerene derivatives in DMSO were mixed with an infection medium (DMEM supplemented with 1% bovine serum albumin, 1% penicillin-streptomycin, and 4 mM L-glutamine) and incubated for 30 min at 37°C under 5% CO_2 [43]. The mixture was added to the cells, and the treated cells were incubated for 24 h at 37°C under 5% CO_2. After incubation, the cells were fixed using a 10% formaldehyde solution. Viable cells were stained with a naphthol blue black solution (0.1% naphthol blue black, 0.1% sodium acetate, and 9% acetic acid) [43].

Immunostaining of Influenza A Virus-infected Cells

MDCK cells were prepared in each well of a 96-well plate. Various concentrations (25–100 μM) of the fullerene derivatives and ME were mixed at a multiplicity of infection (MOI) of 1 influenza A virus (A/PR/8/34 (H1N1) or A/Aichi/2/68 (H3N2)) in the infection medium and incubated for 30 min at 37°C under 5% CO_2. The mixture was added to the cells, and the treated cells were incubated for 24 h at 37°C under 5% CO_2. After incubation, the cells were fixed with 4% paraformaldehyde in phosphate-buffered saline (-) for 30 min at 4°C and then permeabilized with 0.3% Triton X-100 for 20 min at room temperature. A mouse anti-influenza A NP antibody (FluA-NP 4F1; SouthernBiotech, Birmingham, AL, USA) and horseradish peroxidase-conjugated goat anti-mouse IgG antibody (SouthernBiotech) were used as primary and secondary antibodies, respectively [44]. To visualize the infected cells, TrueBlue peroxidase substrate (KPL, Gaithersburg, MD, USA) was added, and color development was terminated after 15 min of incubation by washing with H_2O. The wells were photographed under a microscope, and the stained cells were counted.

Western Blotting

MDCK cells were prepared in each well of a 24-well plate. We mixed 100 μM of the fullerene derivatives and ME at an MOI of 1 influenza A virus (A/PR/8/34 (H1N1)) in the infection medium and incubated the solution for 30 min at 37°C under 5% CO_2. The mixture was added to the cells, and the treated cells were incubated for 4, 8, 12, and 24 h at 37°C under 5% CO_2. After incubation, the cells were lysed with a sodium dodecyl sulfate buffer (125 mM Tris-HCl, pH 6.8, 5% sodium dodecyl sulfate, 25% glycerol, 0.1% bromophenol blue, and 10% β-mercaptoethanol) and boiled for 5 min. The cell lysates were then loaded onto a 10% polyacrylamide gel. The proteins were transferred to a polyvinylidene fluoride microporous membrane (Millipore, Billerica, MA, USA). For primary antibodies, mouse anti-influenza A NP antibody (FluA-NP 4F1; SouthernBiotech) and goat anti-influenza A NS1 antibody (vC-20; Santa Cruz Biotechnology, Santa Cruz, CA, USA) were used to detect NP and NS1, respectively. A rabbit anti-β–actin antibody (13E5; Cell Signaling, Danvers, MA, USA) was used as an internal control. Horseradish peroxidase-conjugated goat anti-mouse IgG antibody (SouthernBiotech), donkey anti-goat IgG antibody (sc-2020; Santa Cruz Biotechnology) and goat anti-rabbit IgG antibody (KPL) were used as secondary Abs. The blots were developed by using Western Lightning ECL Pro (PerkinElmer, Waltham, MA, USA).

Statistical Analysis

All results were expressed as the mean ± standard error of the mean. Differences were analyzed for statistical significance by one-way analysis of variance (ANOVA) for comparison among the DMSO, ME and fullerene derivative-treated groups. The results were considered significantly different at $^{*}p<0.05$ and $^{**}p<0.01$ when comparing the number of stained cells in the ME or fullerene derivatives-treated groups to that of the DMSO-treated group.

Acknowledgments

The influenza A virus (A/PR/8/34 (H1N1)) RNA polymerase PA plasmid, pBMSA-PA, was provided by the DNA bank at the Riken BioResource Center (Tsukuba, Japan; originally deposited by Susumu Nakada) with the support of the National Bio-Resources Project of the Ministry of Education, Culture, Sports, Science, and Technology of Japan.

Author Contributions

Conceived and designed the experiments: TK. Performed the experiments: MS ET DH YI YM RS NE TO. Analyzed the data: MS ET YI YM RS HK. Contributed reagents/materials/analysis tools: SN TM ET HK. Wrote the paper: TK MS.

References

1. Taubenberger JK, Reid AH, Lourens RM, Wang R, Jin G, et al. (2005) Characterization of the 1918 influenza virus polymerase genes. Nature 437: 889–893.
2. Horimoto T, Kawaoka Y (2005) Influenza: lessons from past pandemics, warnings from current incidents. Nat Rev Microbiol 3: 591–600.
3. Hatta M, Gao P, Halfmann P, Kawaoka Y (2001) Molecular basis for high virulence of Hong Kong H5N1 influenza A viruses. Science 293: 1840–1842.

4. Itoh Y, Shinya K, Kiso M, Watanabe T, Sakoda Y, et al. (2009) *In vitro* and *in vivo* characterization of new swine-origin H1N1 influenza viruses. Nature 460: 1021–1025.
5. Neumann G, Noda T, Kawaoka Y (2009) Emergence and pandemic potential of swine-origin H1N1 influenza virus. Nature 459: 931–939.
6. De Clercq E (2006) Antiviral agents active against influenza A viruses. Nat Rev Drug Discov 5: 1015–1025.
7. Hayden FG, Atmar RL, Schilling M, Johnson C, Poretz D, et al. (1999) Use of the selective oral neuraminidase inhibitor oseltamivir to prevent influenza. N Engl J Med 341: 1336–1343.
8. Collins PJ, Haire LF, Lin YP, Liu J, Russell RJ, et al. (2008) Crystal structures of oseltamivir-resistant influenza virus neuraminidase mutants. Nature 453: 1258–1261.
9. Reece PA (2007) Neuraminidase inhibitor resistance in influenza viruses. J Med Virol 79: 1577–1586.
10. Honda A, Ishihama A (1997) The molecular anatomy of influenza virus RNA polymerase. Biol Chem 378: 483–488.
11. Honda A, Mizumoto K, Ishihama A (2002) Minimum molecular architectures for transcription and replication of the influenza virus. Proc Natl Acad Sci U S A 99: 13166–13171.
12. Kuzuhara T, Iwai Y, Takahashi H, Hatakeyama D, Echigo N (2009) Green tea catechins inhibit the endonuclease activity of influenza A virus RNA polymerase. PLoS Curr Oct. 13: 1:RRN1052.
13. Dias A, Bouvier D, Crépin T, McCarthy AA, Hart DJ, et al. (2009) The cap-snatching endonuclease of influenza virus polymerase resides in the PA subunit. Nature 458: 914–918.
14. Yuan P, Bartlam M, Lou Z, Chen S, Zhou J, et al. (2009) Crystal structure of an avian influenza polymerase PA(N) reveals an endonuclease active site. Nature 458: 909–913.
15. Iwai Y, Takahashi H, Hatakeyama D, Motoshima K, Ishikawa M, et al. (2010) Anti-influenza activity of phenethylphenylphthalimide analogs derived from thalidomide. Bioorg Med Chem 18: 5379–5390.
16. Iwai Y, Murakami K, Gomi Y, Hashimoto T, Asakawa Y, et al. (2011) Anti-influenza activity of marchantins, macrocyclic bisbibenzyls contained in liverworts. PLoS One 6: e19825.
17. Kuzuhara T, Kise D, Yoshida H, Horita T, Murazaki Y, et al. (2009) Structural basis of the influenza A virus RNA polymerase PB2 RNA-binding domain containing the pathogenicity-determinant lysine 627 residue. J Biol Chem 284: 6855–6860.
18. Kroto HW, Heath JR, O'Brien SC, Curl RF, Smalley RE (1985) C_{60}: Buckminsterfullerene. Nature 318: 162–163.
19. Sukeguchi D, Singh SP, Reddy MR, Yoshiyama H, Afre RA, et al. (2009) New diarylmethanofullerene derivatives and their properties for organic thin-film solar cells. Beilstein J Org Chem 24: 5–7.
20. Nakamura S, Mashino T (2012) Water-soluble fullerene derivatives for drug discovery. J Nippon Med Sch 79: 248–254.
21. Bosi S, Da Ros T, Spalluto G, Prato M (2003) Fullerene derivatives: an attractive tool for biological applications. Eur J Med Chem 38: 913–923.
22. Mashino T, Shimotohno K, Ikegami N, Nishikawa D, Okuda K, et al. (2005) Human immunodeficiency virus-reverse transcriptase inhibition and hepatitis C virus RNA-dependent RNA polymerase inhibition activities of fullerene derivatives. Bioorg Med Chem Lett 15: 1107–1109.
23. Nishizawa C, Hashimoto N, Yokoo S, Funakoshi-Tago M, Kasahara T, et al. (2009) Pyrrolidinium-type fullerene derivative-induced apoptosis by the generation of reactive oxygen species in HL-60 cells. Free Radic Res 43: 1240–1247.
24. Mashino T, Nishikawa D, Takahashi K, Usui N, Yamori T, et al. (2003) Antibacterial and antiproliferative activity of cationic fullerene derivatives. Bioorg Med Chem Lett 13: 4395–4397.
25. Okuda K, Mashino T, Hirobe M (1996) Superoxide radical quenching and cytochrome c peroxidase-like activity of C_{60}-dimalonic acid, $C_{64}(COOH)_4$. Bioorg Med Chem Lett 6: 539–542.
26. Noble E, Cox A, Deval J, Kim B (2012) Endonuclease substrate selectivity characterized with full-length PA of influenza A virus polymerase. Virology 433: 27–34.
27. DuBois RM, Slavish PJ, Baughman BM, Yun MK, Bao J, et al. (2012) Structural and biochemical basis for development of influenza virus inhibitors targeting the PA endonuclease. PLoS Pathog 8: e1002830.
28. Chemical Computing Group C (2004) Molecular Operative Environment (MOE) 0707.
29. Zhao C, Lou Z, Guo Y, Ma M, Chen Y, et al. (2009) Nucleoside monophosphate complex structures of the endonuclease domain from the influenza virus polymerase PA subunit reveal the substrate binding site inside the catalytic center. J Virol 83: 9024–9030.
30. Tokuyama H, Ymago S, Nakamura E (1993) Photoinduced biochemical activity of fullerene carboxylic acid. J Am Chem Soc 115: 7918–7919.
31. Furuta Y, Takahashi K, Kuno-Mackawa M, Sangawa H, Uehara S, et al. (2005) Mechanism of action of T-705 against influenza virus. Antimicrob Agents Chemother. 49: 981–986.
32. Li L, Chang S, Xiang J, Li Q, Liang H, et al. (2012) Screen anti-influenza lead compounds that target the PA(C) subunit of H5N1 viral RNA polymerase. PLoS One. 7: e35234.
33. Cianci C, Gerritz SW, Deminie C, Krystal M (2012) Influenza nucleoprotein: promising target for antiviral chemotherapy. Antivir Chem Chemother. 10.3851/IMP2235.
34. Ishikawa Y, Fujii S (2011) Binding mode prediction and inhibitor design of anti-influenza virus diketo acids targeting metalloenzyme RNA polymerase by molecular docking. Bioinformation. 6: 221–225.
35. Nakazawa M, Kadowaki SE, Watanabe I, Kadowaki Y, Takei M, et al. (2008) PA subunit of RNA polymerase as a promising target for anti-influenza virus agents. Antiviral Res. 78: 194–201.
36. Tado M, Abe T, Hatta T, Ishikawa M, Nakada S, et al. (2001) Inhibitory effect of modified 5′-capped short RNA fragments on influenza virus RNA polymerase gene expression. Antivir Chem Chemother. 12: 353–358.
37. Nakamura Y, Oda K, Nakada S (1991) Growth complementation of influenza virus temperature-sensitive mutants in mouse cells which express the RNA polymerase and nucleoprotein genes. J Biochem 110: 395–401.
38. Mullis KB, Faloona FA (1987) Specific synthesis of DNA *in vitro* via a polymerase-catalyzed chain reaction. Methods Enzymol 155: 335–350.
39. Studier FW, Moffatt BA (1986) Use of bacteriophage T7 RNA polymerase to direct selective high-level expression of cloned genes. J Mol Biol 189: 113–130.
40. Janknecht R, de Martynoff G, Lou J, Hipskind RA, Nordheim A, et al. (1991) Rapid and efficient purification of native histidine-tagged protein expressed by recombinant vaccinia virus. Proc Natl Acad Sci U S A 88: 8972–8976.
41. Anderson D, Harris R, Polayes D, Ciccarone V, Donahue R, et al. (1996) Rapid generation of recombinant baculoviruses and expression of foreign genes using the Bac-to-Bac® baculovirus expression system. Focus 17: 53–58.
42. Morris GM, Goodsell DS, Halliday RS, Huey R Hart WE, et al. (1998) Automated docking using Lamarckian genetic algorithm and an empirical binding free energy function. J Comp Chem 19: 1639–1662.
43. Goto J, Kataoka R (2008) ASEDock-docking based on alpha spheres and excluded volumes. J Chem Inf Model 48: 583–590.
44. Takahashi E, Kataoka K, Indalao IL, Konoha K, Fujii K, et al. (2012) Oral clarithromycin enhances airway immunoglobulin A (IgA) immunity through induction of IgA class switching recombination and B-cell-activating factor of the tumor necrosis factor family molecule on mucosal dendritic cells in mice infected with influenza A virus. J Virol 86: 10924–10934.

DOI:10.1111/irv.12124
www.influenzajournal.com

Original Article

Intranasal influenza vaccination using a new synthetic mucosal adjuvant SF-10: induction of potent local and systemic immunity with balanced Th1 and Th2 responses

Takashi Kimoto,* Dai Mizuno,* Tsunetomo Takei, Takuya Kunimi, Shinji Ono, Satoko Sakai, Hiroshi Kido

Division of Enzyme Chemistry, Institute for Enzyme Research, The University of Tokushima, Tokushima, Japan.
Correspondence: Hiroshi Kido, Division of Enzyme Chemistry, Institute for Enzyme Research, The University of Tokushima, Tokushima, Japan.
E-mail: kido@ier.tokushima-u.ac.jp
*These two authors contributed equally to this work.

Accepted 24 April 2013. Published Online 26 May 2013.

Background We found previously that bovine pulmonary Surfacten® used in newborns with acute respiratory distress syndrome is a safe and efficacious antigen vehicle for intranasal vaccination.

Objectives The objective of this study was to industrially produce a synthetic adjuvant mimicking Surfacten® for clinical use without risk of bovine spongiform encephalopathy.

Methods We selected three Surfacten lipids and surfactant protein (SP)-C as essential constituents for adjuvanticity. For replacement of the hydrophobic SP-C, we synthesized SP-related peptides and analyzed their adjuvanticity. We evaluated lyophilization to replace sonication for the binding of influenza virus hemagglutinin (HA) to the synthetic adjuvant. We also added a carboxy vinyl polymer (CVP) to the synthetic adjuvant and named the mixture as SF-10 adjuvant. HA combined with SF-10 was administered intranasally to mice, and induction of nasal-wash HA-specific secretory IgA (s-IgA) and serum IgG with Th1-/Th2-type cytokine responses in nasal cavity and virus challenge test were assessed.

Results and Conclusions Intranasal immunization with HA–SF–10 induced significantly higher levels of anti-HA-specific nasal-wash s-IgA and serum IgG than those induced by HA-poly(I:C), a reported potent mucosal vaccine, and provided highly efficient protection against lethal doses of virus challenge in mice. Anti-HA-specific serum IgG levels induced by HA–SF–10 were almost equivalent to those induced by subcutaneous immunization of HA twice. Intranasal administration of HA–SF–10 induced balanced anti-HA-specific IgG1 and IgG2a in sera and IFN-γ- and IL-4-producing lymphocytes in nasal cavity without any induction of anti-HA IgE. The results suggest that HA–SF–10 is a promising nasal influenza vaccine and that SF-10 can be supplied in large quantities commercially.

Keywords influenza vaccine, nasal vaccination, Pulmonary surfactant, synthetic mucosal adjuvant, Th1/Th2 responses.

Please cite this paper as: Kimoto *et al.* (2013) Intranasal influenza vaccination using a new synthetic mucosal adjuvant SF-10: induction of potent local and systemic immunity with balanced Th1 and Th2 responses. Influenza and Other Respiratory Viruses 7(6), 1218–1226.

Introduction

The recent global spread of swine-origin H1N1 influenza A virus (IAV) highlighted the need for the development of effective vaccines for the prevention of viral infection and transmission. The currently available influenza vaccines administered intramuscularly or subcutaneously induce a predominantly IgG-mediated protection in the systemic immune compartment and significantly reduce hospitalization and deaths when they match antigenically the circulating viral strains.[1,2] However, this immunization results in neither adequate induction of antiviral secretory IgA (s-IgA), which provides a wide cross-protection, nor efficient prevention of the initial airway infection[3,4] or cell-mediated responses in the upper and lower respiratory tracts.[5] To address the need for improved influenza vaccines, nasal vaccination that stimulates both mucosal and systemic immunity[4] is desirable for future vaccination against airway viral infection.

Mucosal vaccines and adjuvants have been studied for over 40 years[6,7]; however, many were found to be ineffective or have safety problems.[8] There are two key issues with regard to nasal vaccines.[9] One is the poor efficiency of antigen uptake across the nasal mucosa due to mucociliary clearance. The other is the safety issue; that is, protection against hyperstimulation of antigen-presenting cells or unexpected antibody induction. At present, the cold-adapted live flu mucosal vaccine, FluMist®, is available in the USA[10] for individuals aged 2–49 years and has been licensed in Europe from 2012 under the name FLUENZ for children aged 2–17 years. It is not licensed for children <2 years of age where

it is known to potentially cause post-vaccination flu symptoms with severe wheezing.[11,12]

To overcome these issues, we recently reported that natural pulmonary surfactant and its commercially available bovine product, Surfacten®, which has been used as a natural replacement medicine in premature babies for more than 25 years without significant adverse effects,[13] show safety and efficacy of mucosal adjuvanticities by promoting antigen delivery to antigen-presenting cells in mice and minipigs.[9,14,15] The lung surfactant is effectively uptaked into alveolar cells, macrophages, and dendritic cells and rapidly metabolized *in vivo* with a short half-life of 6–7 hour in the lungs.[16] In addition, we recently found that three major Surfacten lipids and surfactant protein C (SP-C) are essential constituents for mucosal adjuvanticity of Surfacten.[9] In mammals, SP-C is a 33- to 35-residue lipopeptide that consists of a hydrophobic transmembrane α-helix and a cationic N-terminal segment and plays an important role in the uptake of surfactant lipids to alveolar macrophages and epithelial cells.[17] To provide ample supply of the mucosal adjuvant for clinical use, it is important to commercially develop a synthetic compound that carries no risk of bovine spongiform encephalopathy.

In this study, we describe an effective preparation process of a synthetic surfactant (SSF) and a further improved synthetic mucosal adjuvant SF-10 mimicking Surfacten for large-scale manufacturing by improving the following issues. As a substitute for SP-C(1–35), which does not dissolve easily in common organic solvents, we identified a methanol-soluble SP-related peptide. The formation of a complex between influenza hemagglutinin vaccine (HA) and SSF was improved for large-scale manufacturing by lyophilization instead of sonication. In addition, we found a mucoadhesive additive to increase the viscosity of HA-SSF mixture to avoid rapid clearance from the nasal cavity and termed the improved adjuvant compound SF-10. Based on these improvements, we analyzed the enhancement of mucosal and systemic immunity by SF-10 and the resultant Th1- and Th2-type cytokine responses and protective immunity in mice.

Materials and methods

Animals and virus

All experiments were performed in 6- to 8-week-old BALB/c female mice obtained from Japan SLC, Inc. (Shizuoka, Japan). All animals were treated according to the Guide for the Care and Use of Laboratory Animals (NIH Publication No. 85-23, 1996), and the study was approved by the Animal Care Committee of the Tokushima University. IAV/ PR8/34 (H1N1) and A/New Caledonia/20/99(H1N1) were provided by The Research Foundation for Microbial Diseases of Osaka University (Kagawa, Japan).

Reagents

Surfacten® was purchased from Mitsubishi Pharma (Tokyo, Japan). 1,2-Dipalmitoyl-phosphatidylcholine (DPPC), phosphatidylglycerol (PG), and palmitate (PA) for the preparation of SSF were obtained from Nippon Fine Chemical (Osaka, Japan). Synthetic SP-related peptides (Table 1; >80% grade) were obtained from Greiner (Frickenhausen, Germany). A carboxy vinyl polymer (CVP) was purchased from Sigma-Aldrich (St. Louis, MO, USA) and poly(I:C) from Alexis Biochemicals (Lausen, Switzerland).

Preparation of antigen and SSF

IAV/New Caledonia/20/99(H1N1) split antigen (0·2 μg of viral protein, corresponding to 0·14 μg HA; Denka Seiken, Tokyo, Japan) was used as a HA antigen in the present studies. SSF was prepared by mixing three lipids, DPPC, PG, and PA, and various SP-related synthetic peptides, at a molar ratio of 75:25:30:0·6, respectively, as described previously.[9] SSF samples (4 mg phospholipids/ml) were then lyophilized for storage.

Immunization and virus challenge

Lyophilized SSF (its weight was expressed as that of phospholipids) was suspended in distilled water and then mixed with HA (its weight was expressed as protein) in saline at a ratio of 10:1 (wt/wt) as described previously.[9] The SSF–HA complex formation was carried out by sonication or lyophilization. Sonication method[9]: A mixture of SSF and

Table 1. Amino acid sequences of peptides derived from SP-B and SP-C

	Amino acid sequence
SP-B-type peptide	
SP-B (1–25)	FPIPLPYCWLCRALIKRIQAMIPKG
SP-B (20–60)	AMIPKGALAVAVAQVCRVVPLVAGGICQCLAERYSVILLDT
SP-B (64–80)	RMLPQLVCRLVLRCSMD
KL4	KLLLLKLLLLKLLLLKLLLLK
SP-C-type peptide	
SP-C (1–35)	FGIPCCPVHLKRLLIVVVVVLIVVVIVGALLMGL
SP-C (1–12)	FGIPCCPVHLKR
SP-C (1–19)	FGIPCCPVHLKRLLIVVVV
SP-C (13–35)	LLIVVVVVLIVVVIVGALLMGL
SP-CL11	PVHLKRLLLLLLLLLL
SP-CL16	PVHLKRLLLLLLLLLLLLLL
K6L16	KKKKKKLLLLLLLLLLLLLL

HA was treated for 3 minute in a sonic oscillator (model S-250D; Branson Ultrasonics, Danbury, CT, USA) followed by upside-down mixing every 30 minute for 2 hour at room temperature and then stored at 4°C.

Lyophilization method

A mixture of SSF and HA was incubated at 42°C, the critical temperature of Surfacten lipids, for 10 minute with gentle mixing, followed by freezing at −75°C, and then lyophilized. Lyophilized HA + SSF was dissolved in saline before use. Just before administration to mice, CVP in saline at pH 7·0 was added to HA-SSF solution at a final concentration of 0·5%, and the final solution (HA + SSF + CVP) was renamed as HA–SF–10. The amount of HA bound to SSF was calculated by estimating the amount of unbound HA in the SSF-free supernatant fraction after centrifugation as described previously.[9] However, the percentage binding of HA to SF-10 could not be measured due to the inability to separate unbound HA from HA–SF–10 complex by centrifugation or ultrafiltration because of increased viscosity after the addition of CVP.

Mice were immunized by intranasal instillation two or three times every 2 weeks with the prepared samples (2 μl) into each nostril. Positive control mice were subcutaneously injected HA in 100 μl saline under the above immunization schedule. Two weeks after the last immunization, serum and nasal washes were prepared as described previously.[9,14]

For virus challenge experiments, immunized mice were infected with IAV/New Caledonia/20/99(H1N1) at 5×10^4 plaque-forming unit (PFU) by intranasal instillation, for the measurement of neutralization activities of nasal washes. At day 4 after the challenge, virus titers were measured in nasal and lung washes by the plaque assay using Madin-Darby canine kidney cells, which is based on the detection of infected cells using anti-IAV nucleoprotein monoclonal antibody, as described previously.[18]

Immunized mice were also infected with lethal doses of highly pathogenic IAV/ PR8/34(H1N1; 50 and 800 PFU) in 20 μl saline, and the survival rate was monitored for 14 days.

Analysis of mucosal immune responses by ELISA and ELISPOT

Two weeks after the last immunization, serum and nasal-wash specimens were prepared as described previously[14] and subjected to enzyme-linked immunosorbent assay (ELISA) to determine anti-HA-specific s-IgA, IgG, IgG1, IgG2a, and IgE levels.[9,14,15] We used goat anti-mouse IgA, IgG (Sigma, St. Louis, MO, USA), IgG1, IgG2a, or IgE (Bethyl Laboratories, Montgomery, TX, USA) antibodies conjugated with horseradish peroxidase as the secondary antibodies. The levels of total IgE were determined by mouse IgE ELISA Quantitation Set (Bethyl Laboratories). We used 50 ng/ml of purified mouse anti-HA s-IgA, IgG, IgG1, and IgG2a antibodies, which were prepared as described previously,[14] as standards. The hemagglutination inhibition (HI) titers in serum were analyzed after treatment of samples with receptor-destroying enzyme, and the assay was conducted according to the protocol for HI testing established by the World Health Organization, as reported previously.[15]

Mononuclear cells isolated from nasal passages and nasopharynx-associated lymphoid tissue (NALT) by discontinuous Percoll (GE Healthcare, Buckinghamshire, England) density gradient centrifugation[19] were subjected to enzyme-linked immunosorbent spot (ELISPOT) assay, as described previously.[18] The numbers of IL-4- and IFN-γ-producing cells were counted by Mouse ELISPOT Set for IL-4 (BD Pharmingen, Franklin Lakes, NJ, USA) and IFN-γ (MABTECH, Nacka Strand, Sweden) according to the protocols provided by the manufacturers.

Neutralizing activity

To assess the neutralizing activities of the s-IgA in nasal washes, the s-IgA fraction was purified with KAPTIV-AE™ IgA affinity column according to the protocol provided by the manufacturer (Tecnogen, Piacenza, Italy). The concentration of s-IgA was measured by Mouse IgA ELISA Quantitation Set (Bethyl Laboratories). IAV/New Caledonia/20/99(H1N1) at 200 PFU was incubated with 100 μl of the serially diluted s-IgA at 37°C for 1 hour and then the virus titers in the mixtures were measured by the plaque assay, as described previously.[9]

Statistical analysis

All data were expressed as mean ± SD. Differences between groups were examined for statistical significance using the unpaired Student's *t*-test. A P value less than 0·05 denoted statistical significance.

Results

Improvement of synthetic mucosal adjuvant SSF for ample supply

We reported previously that SP-C but not SP-B is an essential constituent of Surfacten for mucosal adjuvanticity.[9] SP-C(1–35) with hydrophobic properties, however, is soluble in 100% trifluoroacetic acid but not in common organic solvents, and its industrial production is scarce. Thus, we designed various peptide fragments of SP-C and SP-B and their modifications (Table 1). SSFs were synthesized by mixing three lipid constituents and each synthetic peptide, and the adjuvanticity was analyzed (Table 2). Adjuvanticity of SSFs containing SP-C-related peptides with 11 to 16 hydrophobic amino acid chain length, but not 7, was almost equivalent to that of Surfacten. Although SSF containing the C-terminal-side hydrophobic domain

Table 2. Effects of mucosal adjuvants, Surfacten, and SSF on the induction of HA-specific antibodies

	Anti-HA antibodies (ng/ml)	
	Nasal washes (s-IgA)	Serum (IgG)
Saline	10·1 ± 4·5	195·5 ± 43·1
HA	9·6 ± 7·4	302·0 ± 125·9
HA-St	196·2 ± 67·7	2907·3 ± 1465·0
HA-SSF		
SP-B type		
SP-B(1–25)	52·0 ± 38·7	622·0 ± 163·9
SP-B(20–60)	37·4 ± 29·4	853·9 ± 344·3
SP-B(64–80)	71·1 ± 37·6	625·9 ± 121·6
KL4	88·3 ± 49·3	778·6 ± 325·9
SP-C type		
SP-C(1–35)	238·1 ± 122·0*	2628·9 ± 942·0*
SP-C(1–12)	23·7 ± 25·5	798·0 ± 688·2
SP-C(1–19)	46·4 ± 40·1	735·1 ± 398·6
SP-C(13–35)	318·1 ± 326·6*	2332·0 ± 1079·7*
SP-CL11	136·6 ± 85·1*	3851·3 ± 2164·1*
SP-CL16	209·8 ± 114·3*	2455·2 ± 1674·3*
K6L16	222·7 ± 145·3*	2104·5 ± 941·7*

Mice were treated with intranasal inoculation of 0·2 μg HA with or without 2 μg of St and various SSF twice at 2-week interval. Two weeks after the last immunization, anti-HA-specific s-IgA in nasal washes and anti-HA-specific IgG in sera were assayed. Data are mean ± SD of 10–15 mice.
*The values are almost equivalent to those of HA-St.

peptide SP-C(13–35) showed relatively high values of anti-HA-specific s-IgA in nasal washes and anti-HA-specific IgG in serum, the levels were not consistent with large SD values. SP-C-related peptides with 11 to 16 hydrophobic amino acid chain length and basic residues in the N-terminal side were soluble in methanol or ethanol, and their adjuvanticity was equivalent to that of Surfacten. Based on these results, we selected a peptide K6L16 among the active peptides, SP-C(1–35), SP-C(13–35), SP-CL11, SP-CL16, and K6L16, as a substitute for SP-C(1–35), which is soluble in methanol and easy for handling, in the following experiments.

To achieve effective antigen delivery, we mixed HA and SSF by sonication to make HA-SSF binding complex. However, avoiding heat damage to HA during sonication is difficult. Accordingly, we used lyophilization as an alternative to sonication and to remove water molecules in the interaction space between HA and SSF for the binding. Lyophilization increased the binding of HA to SSF to ≥92% compared with 65–70% by sonication and significantly increased the induced levels of anti-HA-specific s-IgA in nasal washes at 11·5-fold and IgG in sera at 168·5-fold ($P < 0·01$), compared with those by SSF prepared by sonication (Table 3).

To increase the retention time of HA-SSF in the nasal cavity, we added the mucoadhesive polymer CVP to HA-SSF, to increase its viscosity, at a final concentration of 0·5% just before immunization. The addition of CVP to the lyophilization-prepared HA-SSF further enhanced the induction of anti-HA-specific s-IgA in nasal washes significantly at 4·3-fold ($P < 0·05$) and anti-HA-specific serum IgG at 1·3-fold, the induced levels being the highest among the materials tested. Only limited inductions of anti-HA-specific s-IgA and anti-HA-specific IgG were detected in animals immunized with HA+CPV without SSF, suggesting that SSF is an essential constituent for mucosal adjuvanticity in the mixture. The mixture of HA-SSF and CVP, the best antigen–adjuvant complex, was renamed as HA–SF–10 in the following experiments.

Table 3. Evaluation of various mixing procedures of HA and SSF on induction of HA-specific antibodies

Materials			Preparation			Anti-HA antibodies (μg/ml)	
HA	SSF	CVP	Sonication	Lyophilization	HA binding (%)	Nasal washes (s-IgA)	Serum (IgG)
–	–	–	–	–	-	0·0 ± 0·0	0·1 ± 0·1
+	–	–	+	–	-	0·0 ± 0·0	0·5 ± 0·5
+	+	–	+	–	65-70	0·2 ± 0·2	4·3 ± 0·9
+	+	–	–	+	92-98	2·3 ± 1·4¶	724·5 ± 248·1¶
+	–	+	–	–	-	0·3 ± 0·2	4·9 ± 1·6
+	+	+	+	–	-	3·3 ± 0·9¶	568·7 ± 95·2¶
+	+	+	–	+	-	9·9 ± 5·1¶,*	925·0 ± 633·3¶

Mice were immunized intranasally with HA, with SSF and/or CVP in each combination, three times at 2-week interval. Two weeks after the last immunization, anti-HA-specific s-IgA in nasal washes and IgG in sera were measured by ELISA. Data are mean ± SD of 10–15 mice.
¶$P < 0·01$, compared with HA-SSF mixture prepared by sonication.
*$P < 0·05$, compared with HA-SSF mixture prepared by lyophilization.

Mucosal adjuvanticity of HA–SF–10

For the possible clinical use of SF-10, we evaluated the adjuvanticity of HA–SF–10 and its protective immunity compared with subcutaneously administered HA and intranasally administered HA-poly(I:C), which is one of the most potent mucosal vaccines reported,[20] as positive controls (Figure 1). HA administered subcutaneously twice-effectively induced anti-HA-specific IgG in sera, but not s-IgA in nasal washes. In contrast, intranasally administered HA-SF-10 significantly induced both anti-HA-specific s-IgA in nasal washes and anti-HA-specific IgG in sera, when immunization was repeated three times, compared with the levels induced by intranasal administration of HA or saline three times. No further increase in the induction was observed by administration of HA–SF–10 four times (data not shown). In addition, the levels of anti-HA-specific s-IgA in nasal washes and anti-HA-specific IgG in sera induced by intranasally administered HA–SF–10 were significantly higher at 3·7- and 3·9-fold, respectively, than those induced by intranasally administered HA-poly(I:C) three times ($P < 0·05$). Anti-HA-specific IgG levels in sera induced by intranasal administration of HA–SF–10 three times were almost equivalent to those induced by twice subcutaneous administration of HA. The mean HI titers in serum induced by intranasal administration of HA–SF–10 three times were >300 and were in the similar ranges to those induced by subcutaneous administration of HA twice (Figure S1).

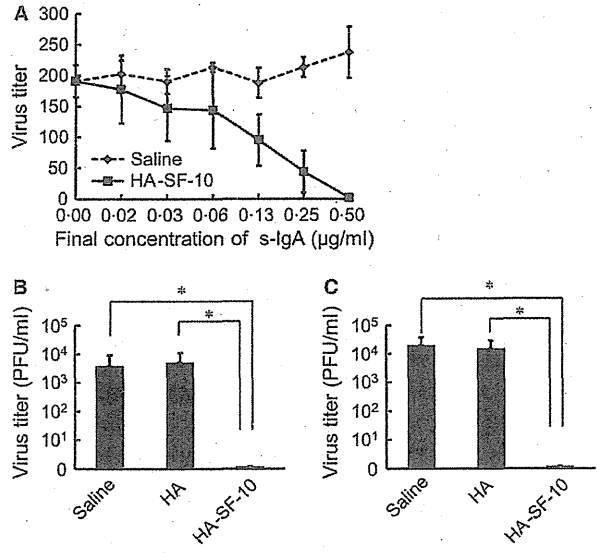

Figure 2. Neutralization activity and protective immunity of nasal washes in mice immunized with intranasal HA–SF–10. (A) Neutralization of IAV/New Caledonia/20/99(H1N1) by isolated s-IgA fraction from nasal washes of mice immunized with intranasal HA–SF–10 or saline. Data are mean virus titer ± SD of three different experiments. (B and C) Two weeks after the last immunization, mice were infected with 5×10^4 PFU of IAV/New Caledonia/20/99(H1N1), and virus titers in nasal washes (B) and lung washes (C) were measured at day 4 after infection. Data are mean ± SD of 8–10 mice. *$P < 0·05$.

Neutralization activities of nasal washes and protective immunity induced by HA–SF–10

In the next step, we assessed the neutralization activities of nasal washes. The neutralizing activity of nasal-wash s-IgA fraction after intranasal immunization with HA–SF–10 is shown in Figure 2A. Nasal-wash s-IgA of mice immunized intranasally with HA–SF–10 neutralized the inoculated IAV/New Caledonia/20/99(H1N1) in a dose-dependent manner, but the fraction obtained from mice treated with saline did not show such activity.

We confirmed the protective immunity in virus challenge experiments (Figure 2B,C). The virus titers in nasal and lung

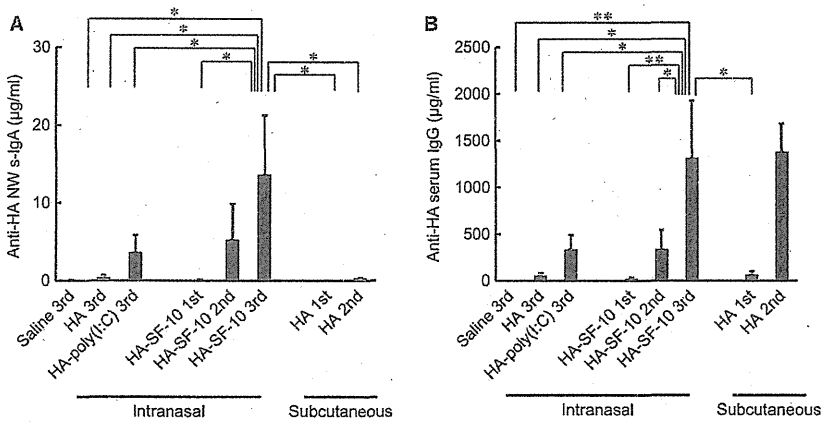

Figure 1. Comparison of the effects of intranasal immunization with HA–SF–10 on mucosal and systemic immunity with those of poly(I:C) and subcutaneous administration of HA. Mice received intranasal HA (0·2 μg) combined with or without SF-10 (2 μg), poly(I:C) (2 μg), or saline, 2 or 3 times every 2 weeks. Another group of mice received subcutaneous HA once or twice every two weeks. After boost inoculation at 2 weeks, the levels of anti-HA-specific s-IgA in nasal washes (NW) (A) and anti-HA-specific IgG in sera (B) were measured. Data are mean ± SD of 5–10 mice. *$P < 0·05$, **$P < 0·01$.

washes were measured after 4-day infection of immunized mice with 5×10^4 PFU of IAV/New Caledonia/20/99 (H1N1). High virus titers were detected in mice immunized with saline or intranasal HA. In contrast, the virus titer was below the detection limit in both nasal and lung washes of mice immunized intranasally with HA–SF–10. We also assessed the protective immunity in mice challenged with two lethal doses ($10 \times LD_{50}$, 50 PFU and $160 \times LD_{50}$, 800 PFU) of IAV/PR8/34(H1N1), a similar subtype but highly pathogenic strain of IAV (Figure 3). All mice that were immunized intranasally with HA–SF–10 survived against the infection with $10 \times LD_{50}$ of IAV/PR8/34(H1N1), but all mice that were immunized with intranasal HA or saline died at day 10. About 80% of mice immunized twice with subcutaneous HA died at day 8 (Figure 3A). Even in more severe virus challenge, 90% of mice immunized with intranasal HA–SF–10 survived against infection with $160 \times LD_{50}$ of IAV/PR8/34(H1N1), while only 10% of mice immunized intranasally with HA-poly(I:C) and none of those immunized intranasally with HA or saline survived (Figure 3B).

Induction of HA-specific Th1- and Th2-type immune responses by HA–SF–10

To assess the effect of intranasal administration of HA–SF–10 on T-helper responses, we analyzed the subclasses of anti-HA-specific IgG (IgG1 and IgG2a) as well as IgE in sera and the induction of Th1- and Th2-type cytokine responses in mucosal lymphoid tissues. Intranasal immunization with HA–SF–10 induced not only anti-HA-specific IgG1 and Th2-type antibody, but also anti-HA-specific IgG2a and Th1-type antibody, and these levels suggested a balanced Th1/Th2 response (Figure 4A). The induced levels of IgG1 and IgG2a by intranasal administration of HA-SF-10 were significantly higher than those by HA-poly (I:C) ($P < 0{\cdot}01$ and $P < 0{\cdot}05$, respectively). However, the mean serum IgG2a/IgG1 ratio in mice immunized intranasally with HA–SF–10 was comparable with that of mice immunized with HA-poly(I:C) (Figure 4B). On the other hand, the mean serum IgG2a/IgG1 ratio was significantly low in mice immunized subcutaneously with HA compared with the value induced by HA–SF–10 ($P < 0{\cdot}05$).

Finally, we analyzed anti-HA-specific IgE (Figure 4C) and total IgE levels (Figure 4D) to exclude allergic responses after intranasal immunization with HA–SF–10. None of the mice immunized intranasally with HA–SF–10 showed the induction of anti-HA-specific IgE or total IgE in the serum, although distinct induction by subcutaneous administration of HA was detected. We also studied the expression levels of IFN-γ (Th1-associated cytokine) and IL-4 (Th2-associated cytokine) in mucosal lymphoid tissues of mice, such as NALT and nasopharynx, by ELISPOT (Figure 5). Mice immunized intranasally with HA–SF–10 showed significantly higher induction of both IL-4- and IFN-γ-producing cells than the induction of mice immunized intranasally with HA or saline. The numbers of induced IL-4- and IFN-γ-producing cells were higher in nasopharynx than those in NALT. The number of induced IL-4-producing cells and IFN-γ-producing cells supports the results of the balanced serum IgG2a/IgG1 ratio shown in Figure 4.

Discussion

Many potential mucosal adjuvants have been evaluated in the past, but no safe and efficacious mucosal adjuvant is available commercially at present. To overcome these issues, we recently reported a bovine pulmonary surfactant that enhances antigen delivery to dendritic cells, increases antigen sustainability in the nasal cavity, and induces both mucosal and systemic immunity.[9,14,15] To provide ample supply of this adjuvant without any risk of bovine spongiform encephalopathy, we prepared synthetic SSF, which comprises three major lipids, and synthetic human SP-C(1–35), resembling the natural surfactant.[9] Although the mucosal adjuvanticity of SSF is almost equivalent to that of natural Surfacten, there are four major problems that curtail the use

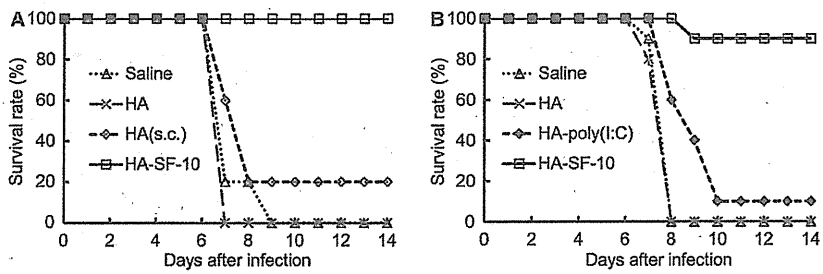

Figure 3. Survival rates of immunized mice after infection with lethal doses of IAV/PR8/34(H1N1) virus. (A) Mice were immunized with intranasal HA (0·2 μg) combined with or without SF-10 (2 μg), polyc (I:C) (2 μg) or saline three times every 2 weeks. Another group of mice received subcutaneous (s.c.) HA twice every two weeks. Two weeks after the last immunization, mice were infected with $10 \times LD_{50}$ (50 PFU) (A) and $160 \times LD_{50}$ (800 PFU) (B) of IAV/PR8/34(H1N1) virus, and their survival rates were monitored.